RESEARCH ARTICLE

National Science Review
8: nwaa269, 2021
https://doi.org/10.1093/nsr/nwaa269
Advance access publication 24 October 2020

PHYSICS

Synchronization within synchronization: transients and intermittency in ecological networks

Huawei Fan[1,2], Ling-Wei Kong[2], Xingang Wang[1], Alan Hastings[3,4] and Ying-Cheng Lai[2,5,*]

ABSTRACT

Transients are fundamental to ecological systems with significant implications to management, conservation and biological control. We uncover a type of transient synchronization behavior in spatial ecological networks whose local dynamics are of the chaotic, predator–prey type. In the parameter regime where there is phase synchronization among all the patches, complete synchronization (i.e. synchronization in both phase and amplitude) can arise in certain pairs of patches as determined by the network symmetry—henceforth the phenomenon of 'synchronization within synchronization.' Distinct patterns of complete synchronization coexist but, due to intrinsic instability or noise, each pattern is a transient and there is random, intermittent switching among the patterns in the course of time evolution. The probability distribution of the transient time is found to follow an algebraic scaling law with a divergent average transient lifetime. Based on symmetry considerations, we develop a stability analysis to understand these phenomena. The general principle of symmetry can also be exploited to explain previously discovered, counterintuitive synchronization behaviors in ecological networks.

Keywords: ecological networks, cluster synchronization, phase synchronization, transient chaos, network symmetry

[1]School of Physics and Information Technology, Shaanxi Normal University, Xi'an 710062, China; [2]School of Electrical, Computer and Energy Engineering, Arizona State University, Tempe, AZ 85287, USA; [3]Department of Environmental Science and Policy, University of California, Davis, CA 95616, USA; [4]Santa Fe Institute, Santa Fe, NM 87501, USA and [5]Department of Physics, Arizona State University, Tempe, AZ 85287, USA

***Corresponding author.** E-mail: Ying-Cheng.Lai@asu.edu

Received 5 June 2020; **Revised** 28 September 2020; **Accepted** 28 September 2020

INTRODUCTION

Synchronization in spatially extended ecological systems has been a topic of continuous interest [1–14]. In a variety of ecosystems, cyclic patterns across space that persist in time are ubiquitous, in which synchronous dynamics are believed to play an important role [2,3,11,14]. For example, in a network of predator–prey systems, chaotic phase synchronization was uncovered, providing an explanation for a class of ecological cycles, e.g. the hare-lynx cycle [15–19], in which the populations in different spatial regions oscillate synchronously and periodically in phase but their peak abundances are different and vary erratically with time [2,3]. More recently, synchronous dynamics were exploited to explain the correlations across space of cyclic dynamics in ecology, especially in terms of yield from pistachio trees [11,14]. Based on a large data set from over 6500 trees in a pistachio orchard in California, the authors established a surprising link between the spatially networked system of pistachio trees and the Ising model in statistical physics, with the common trait that local, neighbor-to-neighbor interactions (root grafting for the former and spin interactions for the latter) can generate correlation and synchronization over large distances.

In ecology, the importance of transient dynamics has been increasingly recognized [20–24], making uncovering and understanding ecological transients a frontier area of research [25]. In this paper, we report a class of transient synchronization behaviors in a spatially distributed ecological network of patches, each with a chaotic predator–prey type of dynamics. The oscillators are locally coupled and, for simplicity, they are located on a topological circle in space. Each oscillator describes the population dynamics of a patch, in which there are three interacting species: vegetation, herbivores and predators. When isolated, the dynamics of the oscillators are chaotic. In the presence of local coupling, chaotic phase synchronization prevails [2,3,26]. Our main finding is that, enclosed within phase synchronization, complete synchronization in both phase and amplitude of the abundance oscillations emerges among certain subsets of patches. The subsets are determined by the intrinsic symmetries of the network, i.e. each symmetry generates a specific configuration of the subsets (or clusters of oscillators). There is then cluster synchronization. As complete synchronization among a subset of patches occurs under the umbrella of phase synchronization among *all* the patches, we call this phenomenon 'synchronization within synchronization.' The striking behavior is that the synchronous dynamics associated with any configuration are *transient*: any cluster synchronization can be maintained for only a finite amount of time when the network is subject to intrinsic stochasticity (due to chaos) and/or random noise of arbitrarily small amplitude. When one form of cluster synchronization breaks down, a new form of cluster synchronization allowed by the system symmetry emerges. In the course of time evolution, there is intermittent switching among the distinct patterns of cluster synchronization. The duration of any cluster synchronization state, or the transient time, is found to obey an algebraic scaling law. Mathematically, the emergence of transient cluster synchronization, intermittency and the distribution of the transient lifetime can be understood through a dynamical stability analysis based on symmetry considerations. Ecologically, in addition to uncovering transients in patch synchronization dynamics, our finding implies that the ubiquitous phenomenon of population cycles can possess a more organized dynamical structure than previously thought: not only do the populations in all patches exhibit the same trend of variation (synchronized in phase), but certain patches can also have the same population at any time even if they are not directly coupled and are separated by a large distance. In fact, nearby patches, in spite of being directly coupled, may not be completely synchronized. The results establish the possibility and the dynamical mechanism for spatially 'remote' synchronization in ecological systems.

We remark that, in the field of complex dynamical systems, the phenomenon of cluster synchronization has been investigated [27–30]. For example, it was found earlier that long-range links added to a loop network can induce cluster synchronization patterns [27]. Removing links or adding weights to links can affect the stability of cluster synchronization and induce switching among different patterns of synchronization [28]. In a symmetric network of coupled identical phase oscillators, phase lags can induce cluster synchronization [29]. These previous studies established a fundamental connection between the symmetry of the network and the patterns of cluster synchronization, and a computational group theory was developed [30] to understand this connection. For example, a group can be generated by the possible symmetries of a network and the orbits of the symmetry group determine the partition of the synchronous clusters. In general, the phase space of the whole networked dynamical system can be decomposed into the synchronization subspace and the transverse subspace through a transformation matrix generated by the symmetry group, which determines the stability of the cluster synchronization patterns. In the existing literature on cluster synchronization, there are two common features: (1) the clusters are desynchronized from each other, in both phase and amplitude, and (2) a cluster synchronization state is sustained. In addition, the phenomenon of intermittent synchronization was studied, where the system switches between cluster and global synchronizations [31], a phenomenon that is usually induced by noise [32]. Quite distinctively, the transient cluster synchronization state uncovered in this paper has the following features. (1) The clusters are synchronized in phase, and (2) the emergence of the cluster configuration is time dependent and in fact transient: it can alter in an intermittent fashion where the system switches between different cluster synchronization states. To our knowledge, the phenomena uncovered in this paper, namely transient cluster synchronization umbrellaed by chaotic phase synchronization and intermittent switching among the coexisting cluster synchronization patterns, were not known previously. The phenomena enrich our knowledge about the interplay between network symmetry and the collective dynamics, and are broadly interesting to researchers from different fields including physics, complex systems and ecology.

RESULTS

We consider the following vertical food web network model [2]:

$$\dot{x}_i = a x_i - \alpha_1 f_1(x_i, y_i), \tag{1a}$$

$$\dot{y}_i = -b y_i + \alpha_1 f_1(x_i, y_i) - \alpha_2 f_2(y_i, z_i) + \varepsilon_y \sum_{j=1}^{N} a_{ij}(y_j - y_i), \tag{1b}$$

$$\dot{z}_i = -c(z_i - z_0) + \alpha_2 f_2(y_i, z_i) + \varepsilon_z \sum_{j=1}^{N} a_{ij}(z_j - z_i). \tag{1c}$$

Here $i, j = 1, \ldots, N$ are the oscillator (patch) indices, and the dynamical variables x_i, y_i and z_i represent

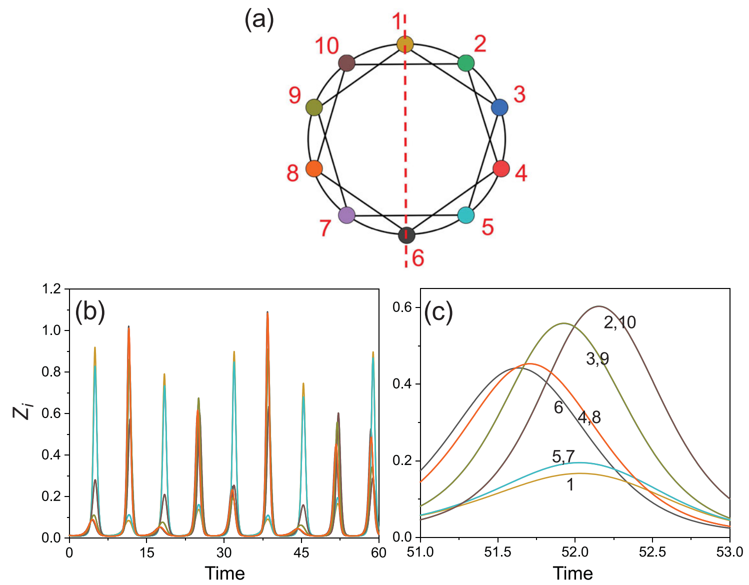

Figure 1. Network structure, chaotic phase synchronization, and evidence of cluster synchronization. (a) A dispersal network of ten patches with a regular ring structure. Each node has four links: two to the nearest neighbors and two to the next nearest neighbors. The red dashed line specifies the symmetry axis. (b) Representative time series of the ten predator populations z_i for $\varepsilon = 0.038$. The phases of the chaotic oscillators are synchronized, as the peaks of all predator populations are locked with each other. (c) A magnification of a single peak of the time series in (b), where there are six distinct time series, indicating that the four remaining time series coincide completely with some of the six distinct time series. In fact, there are four pairs of patches, (2,10), (3,9), (4,8) and (5,7), and both the amplitude and phase of the paired patches are synchronized—complete synchronization, signifying network cluster synchronization.

the abundances of vegetation, herbivores and predators in patch i, respectively. The consumer–resource and predator–prey interactions are represented by the Holling type-II term $f_1(x, y) = xy/(1 + \beta x)$ and the Lotka-Volterra term $f_2(y, z) = yz$, respectively. For the parameter setting $(a, b, c, z_0, \alpha_1, \alpha_2, \beta) = (1, 1, 10, 6 \times 10^{-3}, 0.2, 1, 5 \times 10^{-2})$, the local dynamics of each patch display the feature of uniform phase growth and chaotic amplitude commonly observed in ecological and biological systems [33]. In fact, with this set of parameter values, the individual isolated nodal dynamics reproduce the time series of lynx abundances observed from six different regions in Canada during the period from 1821 to 1934 [2]. The patches are coupled through the migrations of herbivores (y) and predators (z), with the respective coupling parameters ε_y and ε_z. The coupling relationship of the patches, namely the network structure, is described by the adjacency matrix $A = \{a_{ij}\}$: $a_{ij} = a_{ji} = 1$ if patches i and j are connected; otherwise, $a_{ij} = 0$. Ecologically, food web networks usually are not large [2,34]. Following the setting in [34], we study a small regular ring network of $N = 10$ discrete habitat patches, as illustrated in Fig. 1(a). The phenomenon to be reported below also occurs for different parameter values, e.g. for $0.7 \le b \le 1.2$.

Emergence of cluster synchronization

We focus on the case in which $\varepsilon_y = \varepsilon_z \equiv \varepsilon$. (The general case of $\varepsilon_y \neq \varepsilon_z$ is treated in Section I of the online supplementary material [SM]) It was shown previously [2] that, while the species in different patches exhibit chaotic variations, phase synchronization among the populations in all patches can arise. That is, the populations exhibit exactly the same trend of ups and downs, giving rise to certain degree of spatial correlation or coherence. An example of chaotic phase synchronization is shown in Fig. 1(b), where the time series of the predator species z_i in all patches are displayed. It can be seen that the highs of the ten populations occur in the same time intervals, so are the lows. The amplitudes of the population variations are chaotic and apparently not synchronized. If there is an absolute lack of any synchronization in amplitude, the ten time series should all have been distinct. However, a careful examination of the time series reveals fewer than ten distinct traces; as shown in Fig. 1(c), there are only six distinct time series, among which the population amplitudes of the following four pairs of patches are completely synchronized: (5,7), (4,8), (3,9), (2,10) (patch 1 is not synchronized in amplitude with any other patch, neither is patch 6). The remarkable phenomenon is the emergence of complete synchronization in both phase and amplitude between patches that are not directly coupled with each other, such as patches 4 and 8 as well as 3 and 9. For any one of these four patches, its population chooses to synchronize not with that of the nearest neighbor or that of the second nearest neighbor (i.e. a directly coupled patch), but with that of a relatively remote one. That is, for the coupled chaotic food web network, while previous work [2,3] revealed that the populations of all spatial patches vary coherently in phase, a stronger level of coherence, i.e. synchronization in both phase and amplitude, can emerge spontaneously between spatially remote patches.

Intermittency associated with cluster synchronization

To characterize cluster synchronization within chaotic phase synchronization, we define the following synchronization matrix $\mathcal{C}(t)$ with element $c_{ij}(t)$: $c_{ij}(t) = c_{ji}(t) = 1$ if the difference between the predator populations of patches i and j is sufficiently small, e.g. $|z_j(t) - z_i(t)| < 10^{-4}$, and $c_{ij}(t) = 0$ otherwise. As shown in the top row of Fig. 2, for

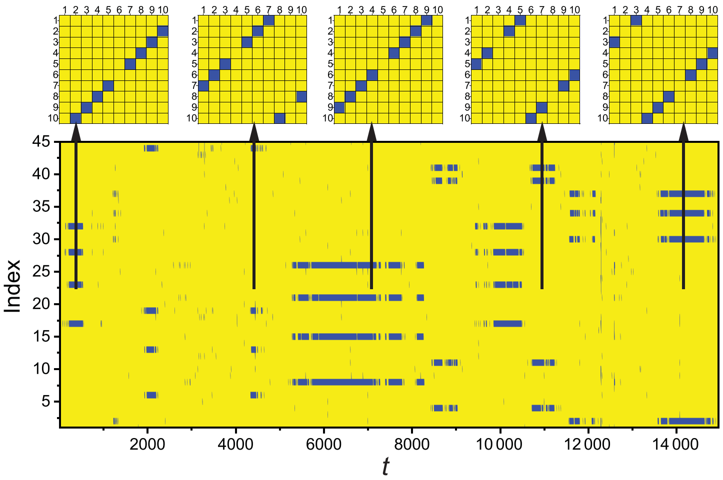

Figure 2. Cluster synchronization within chaotic phase synchronization and intermittent switching. Shown is the time evolution of the matrix elements $c_{ij}(t)$ for $\varepsilon = 0.038$, where the elements of one are marked blue and the others are marked yellow. In the top panel, there are five distinct matrices, indicating five cluster synchronization states or patterns. The corresponding time series are displayed in the bottom panel. The index marks the element position of the upper triangular part of c_{ij} and time t is rescaled by the average period of the population oscillations. Each vertical arrow indicates the time interval in which a specific cluster synchronization state appears.

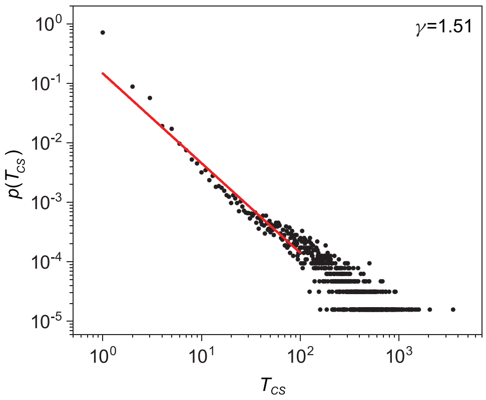

Figure 3. Probability distribution of the transient lifetime—the time for the network to maintain a specific cluster synchronization state. Shown is the probability distribution function $p(T_{CS})$ for $\varepsilon = 0.038$, where T_{CS} denotes the transient lifetime. The distribution can be fitted by an algebraic scaling: $p(T_{CS}) \sim T_{CS}^{-\gamma}$ with $\gamma \approx 1.51$.

$\varepsilon = 0.038$, there are five distinct states of cluster synchronization, where for each state (panel), the blue squares signify complete synchronization between patches i and j with $c_{ij} = 1$, and the yellow squares are amplitude desynchronized pairs with $c_{ij} = 0$. For example, for the leftmost panel, the amplitude-synchronized pairs are (5,7), (4,8), (3,9) and (2,10), which correspond to the time series in Fig. 1(b) and (c). Examining the network structure in Fig. 1(a), we see that this state of cluster synchronization is induced by a specific reflection symmetry: one whose axis of symmetry is the line connecting nodes 1 and 6. In fact, each of the four other distinct cluster-synchronization states is generated by a different reflection symmetry of the network, with their symmetry axes being (4,9), (5,10), (3,8) and (2,7), respectively. The bottom panel in Fig. 2 shows the evolution of c_{ij} in a long time interval of approximately 15 000 average periods, where the ordinate specifies the position of the matrix element c_{ij}. Note that, because of the symmetry of the matrix and the trivial diagonal elements, only the elements in the upper triangular part of the matrix are shown. To be specific, the position index of c_{ij} (with $j > i$) is calculated as $I = (j - i) + \sum_{i'=1}^{i-1} \sum_{j'=i'+1}^{N} 1$. There are in total 45 positions in the bottom panel of Fig. 2. In the course of time evolution, there is intermittent switching of the cluster synchronization state. That is, a cluster synchronization state can sustain but only for a finite amount of time and then becomes unstable, after which a short time interval of desynchronization arises. At the end of the desynchronization epoch, the system evolves spontaneously into a randomly chosen cluster synchronization state that could be distinct from the one before the desynchronization epoch. Figure 2 thus indicates that each possible cluster synchronization state enabled by the network symmetry is transient, and the evolution of cluster synchronization within phase synchronization is intermittent.

Figure 2 indicates that the time to maintain a specific cluster state, or the transient lifetime denoted as T_{CS}, is irregular. Through Monte Carlo simulation of the network dynamics with a large number of initial conditions, we obtain the probability distribution of T_{CS}, as shown in Fig. 3 for $\varepsilon = 0.038$. The distribution is approximately algebraic: $p(T_{CS}) \sim T_{CS}^{-\gamma}$ with the exponent $\gamma \approx 1.51$. The algebraic distribution indicates that an arbitrarily long transient of cluster synchronization can occur with a nonzero probability and, because the value of the exponent is between one and two, the average transient lifetime diverges.

Dynamical mechanism of intermittency—effect of noise

The five distinct cluster synchronization states enabled by the symmetries of the network, as demonstrated in Fig. 2, are coexisting asymptotic states (or attractors) of the system. That is, the ecological network (1) exhibits multistability, a ubiquitous phenomenon in nonlinear dynamical systems [35–43]. The numerically observed behavior of intermittency

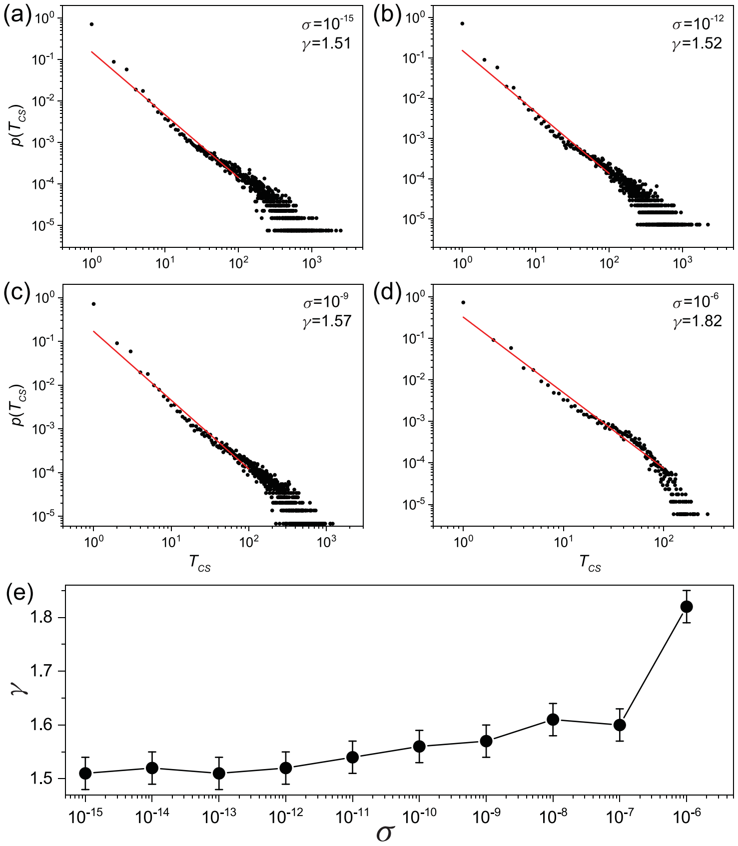

Figure 4. Effect of noise on the algebraic distribution of the transient lifetime of the cluster synchronization state. (a)–(d) Algebraic distribution $p(T_{CS})$ for four values of the noise amplitude σ: 10^{-15}, 10^{-12}, 10^{-9} and 10^{-6}. The values of the algebraic exponent are approximately 1.51, 1.52, 1.57 and 1.82, respectively. Larger noise reduces (often significantly) the probability of a long transient lifetime. (e) An increasing trend of the algebraic exponent γ with noise amplitude σ.

in Fig. 2 is effectively random hopping among the coexisting attractors induced by computational 'noise.' To see this, consider the regime of the coupling parameter where the cluster synchronization state is weakly stable (to be defined precisely below) and imagine simulating the system dynamics using an infinitely accurate algorithm on an ideal machine with zero round-off error. In this idealized setting, from a given set of initial conditions, the system dynamics will approach an attractor corresponding to a specific cluster synchronization state. Because of absence of error or noise of any sort, the system will remain in this attractor indefinitely. Realistically, inevitable random computational errors will 'kick' the system out of the attractor and settle it into another attractor corresponding to a different cluster synchronization state but for a finite amount of time, kick it out again, and so on, generating an intermittent hopping or switching behavior as demonstrated in Fig. 2.

To provide support for this mechanism of intermittency, we investigate the effect of deliberately supplied noise on intermittency. In particular, we assume that system equation (1) is subject to additive, independent, Gaussian white noise $\eta(t)$ at each node for each dynamical variable (x, y, or z), with $\langle\eta(t)\rangle = 0$ and $\langle\eta(t)\eta(t')\rangle = \sigma^2\delta(t-t')$, where σ is the noise amplitude and $\delta(x)$ is the Dirac delta function. We calculate the distributions of the transient lifetime for different noise levels. The idea is that, when the noise amplitude is smaller than or comparable to the computational error (about 10^{-15}), the algebraic distribution should be similar to that without external noise with a similar exponent to that in Fig. 3, i.e. about 1.5. Stronger noise will induce more frequent switching and reduce the probability of a long transient time, giving rise to a larger exponent. Evidence for this scenario is presented in Fig. 4, where we observe that a larger noise amplitude indeed leads to a larger value of the algebraic scaling exponent γ. For variation of noise amplitude over nine orders of magnitude (from 10^{-15} to 10^{-6}), the lifetime distribution $p(T_{CS})$ remains robustly algebraic, and the value of the algebraic exponent γ increases from about 1.5 to 1.8. For example, for $\sigma = 10^{-15}$, there are long lifetime intervals over 1000 (average cycles of population oscillation). However, for $\sigma = 10^{-6}$, no such intervals have been observed.

Evidence of generality: transient cluster synchronization in the Hastings–Powell model

To demonstrate the generality of the phenomena of transient cluster synchronization and intermittency, we consider the Hastings–Powell model of a chaotic food web network [44]:

$$\dot{x}_i = x_i(1-x_i) - f_1(x_i)y_i, \tag{2a}$$

$$\dot{y}_i = f_1(x_i)y_i - f_2(y_i)z_i - d_1y_i + \varepsilon_y\sum_{j=1}^{N} a_{ij}(y_j - y_i), \tag{2b}$$

$$\dot{z}_i = f_2(y_i)z_i - d_2z_i + \varepsilon_z\sum_{j=1}^{N} a_{ij}(z_j - z_i). \tag{2c}$$

Here the index $i = 1, 2, \ldots, N$ denotes the individual patches, x is the population of species at the lowest level of the food chain, and y and z are the populations of the species that prey on x and y, respectively. The nonlinear functions $f_l(w)$ are given by $f_l(w) = a_lw/(1+b_lw)$, and the representative parameter values [44] are $a_1 = 5.0$, $a_2 = 0.1$, $b_1 = 3.0$, $b_2 = 2.0$, $d_1 = 0.4$ and $d_2 = 0.01$. (The phenomenon

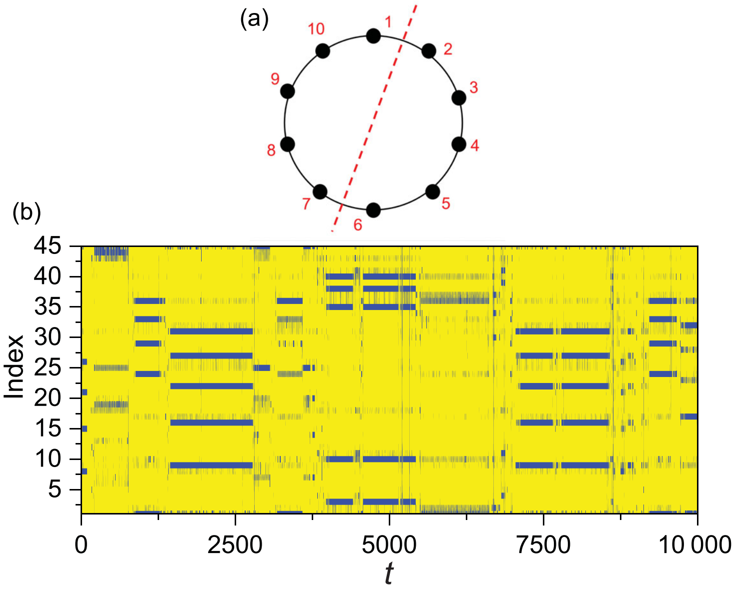

Figure 5. Network structure and intermittent cluster synchronization in the Hastings–Powell model. (a) A dispersal network of ten patches with a regular ring structure. The red dashed line specifies one of the five symmetry axes that lead to five possible cluster synchronization states of patterns. (b) Representative time evolution of the matrix elements $c_{ij}(t)$ for $\varepsilon = \varepsilon_y = \varepsilon_z = 0.00869$. The time is rescaled by the average period of the population oscillations.

of transient cluster synchronization to be reported also occurs for other parameter values, e.g. when d_1 varies in the interval $[0.35, 0.4)$.) Pairwise linear coupling occurs between the y and z variables with the corresponding coupling parameters ε_y and ε_z.

We study a locally coupled, regular ring network of $n = 10$ patches, as shown in Fig. 5(a). Representative time evolution of the matrix elements c_{ij} is shown in Fig. 5(b) for $\varepsilon = \varepsilon_y = \varepsilon_z = 0.00869$, where time t is rescaled by the average period of the population oscillations. To facilitate observation of cluster synchronization, we define the synchronization matrix element $c_{ij}(t)$ as $c_{ij}(t) = c_{ji}(t) = 1$ if the difference between the populations z of patches i and j remains sufficiently small within one natural period T of the population oscillation: $|z_i(t) - z_j(t)| < 2.0 \times 10^{-2}$ for $t \in T$, and $c_{ij}(t) = 0$ otherwise. Similar to Fig. 2, there is intermittent cluster synchronization in the Hastings–Powell model as well. In Fig. 6 we show the probability distributions of T_{CS} for different values of the noise amplitude, which are similar to the results in Fig. 4.

DISCUSSION

Focusing on small, chaotic dispersal networks with relatively strong interactions and a regular structure, we have uncovered a type of transient ecological dynamics in terms of synchronization. In particular, in the parameter regime beyond weak coupling where there is phase synchronization among all the patches but the interactions are not strong enough for global synchronization in both phase and amplitude among all patches, transient amplitude synchronization between the symmetric patches can arise. (Phase synchronization occurs in the regime of weak coupling, yet no cluster phase synchronization has been observed about the transition point.) The emergence of cluster synchronization in amplitude within phase synchronization represents a remarkable organization of synchronous dynamics in ecological networks. Each symmetry in the network structure generates a distinct cluster synchronization pattern. Multiple symmetries in the network lead to multiple coexisting cluster synchronization patterns (attractors). Because of instability and noise, each cluster synchronization pattern can last for a finite amount of time, leading to random, intermittent switching among the coexisting patterns. The transient time during which a particular cluster synchronization pattern can be maintained follows an algebraic probability distribution. General symmetry considerations enable us to define the cluster synchronization manifold and to quantify its stability by calculating the largest transverse Lyapunov exponent (see the Methods section and Section I of the SM). Finite-time fluctuations of this exponent into both the positive and negative sides are key to understanding the intermittent behavior. A strong similarity to random walk dynamics provides a natural explanation of not only the algebraic nature of the transient lifetime distribution but also the value of the algebraic exponent. Alterations in the structure of the network do not affect these results. For example, we have studied a one-dimensional ring network with an odd number of patches and a spatially two-dimensional lattice, and found that the phenomena of cluster synchronization in amplitude shadowed by chaotic phase synchronization and intermittency persist (see Sections IV and V of the SM). In addition, factors such as variations in coupling strength (see Sections II and VI of the SM) and local parameters (see Section VIII of the SM), noise perturbations (see Section VII of the SM), and symmetry perturbations (see Section XIII of the SM) do not significantly alter the phenomenon.

Our stability analysis has revealed the fundamental role played by network symmetry in the emergence of transient cluster synchronization and intermittency. Symmetry considerations can also be used to explain intriguing, counterintuitive synchronization phenomena in ecological networks. For example, in a previous work on a class of dispersal ecological networks, essentially a nondimensional

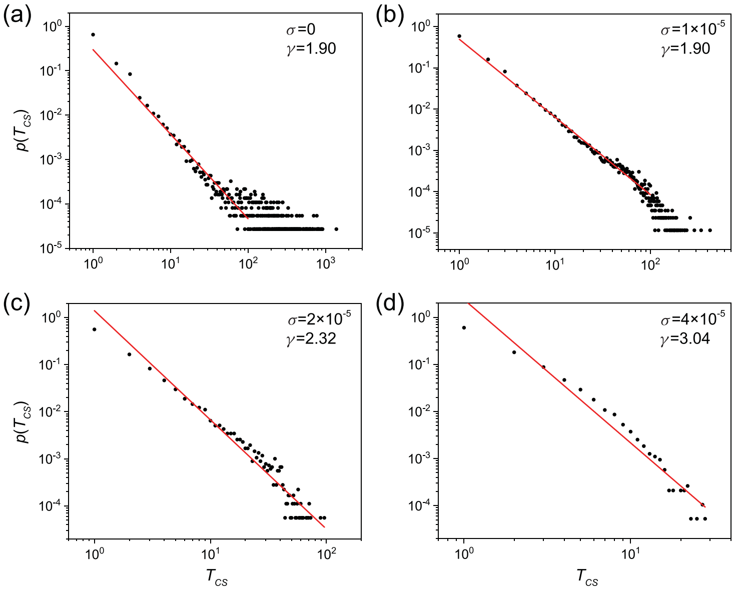

Figure 6. Effect of noise on the algebraic distribution of the transient lifetime of the cluster synchronization state in the Hastings–Powell model. (a)–(d) Algebraic distribution $p(T_{CS})$ for four values of the noise amplitude σ: 0, 1×10^{-5}, 2×10^{-5} and 4×10^{-5}, respectively.

and spatially structured form of the Rosenzweig–MacArthur predator–prey model [45], it was found that the dispersal network structure has a strong effect on the ecological dynamics in that randomizing the structure of an otherwise regular network tends to induce desynchronization with prolonged transient dynamics [34]. This contrasts the result in the literature of complex networks where synchronization is typically favored by creating random shortcuts in a large regular network, i.e. by making the network structure the small-world type [46–48]. The paradox is naturally resolved by resorting to symmetry. In particular, in the small regular network studied in [34], the observed cluster synchronization patterns are the result of the reflection symmetries of the network. Adding random shortcuts destroys certain symmetry and, consequently, the corresponding synchronization pattern.

In realistic ecological networks, both the dynamics of the patches and the interactions among them can be nonidentical. As the formation of synchronous clusters relies on the network symmetry, a natural question is whether transient cluster synchronization can be observed in ecological networks of nonidentical oscillators and heterogeneous interactions. One approach to addressing this is to introduce perturbations, e.g. parameter and coupling perturbations, to the system and to test if transient cluster synchronization persists. Our computations provided an affirmative answer (see Section XIII of the SM). The results are consistent with the previous findings in the physics literature, where stable cluster synchronization persists when the network symmetries are slightly broken or when the oscillator parameters are slightly perturbed [30,49,50]. Besides ecological networks, we have also observed transient cluster synchronization in the network of coupled chaotic Rössler oscillators (see Section IX of the SM), suggesting the generality of the phenomenon. Whether this phenomenon can arise in large-scale complex networks with heterogeneous nodal dynamics is an open question worth pursuing.

The importance of transients in ecological systems has been increasingly recognized [20–25]. Our work has unearthed a type of transient behavior in the collective dynamics of ecological systems: a synchronization pattern can last for a finite amount of time and be replaced by a completely different pattern in a relatively short time. The finding of transient synchronization dynamics may have implications to ecological management and conservation, and provide insights into experimental observations. For instance, in a recent experiment on the planktonic predator–prey system [51], it was shown that, whereas the abundances of the predator and prey display mostly regular and coherent oscillations, short episodes of irregular and noncoherent oscillations can arise occasionally, making the system switch randomly among different patterns. Furthermore, controlled experiments and simulation of the mathematical model suggest that the switching behavior can be attributed to the intrinsic stochasticity of the system dynamics. The switching behavior reported in [51] is quite similar to the phenomenon of transient, intermittent cluster synchronization uncovered here. As pointed out in [52], the key to explaining the experimentally observed phenomenon is to uncover the role of transient dynamics—the main question that has been addressed in our present work. The findings reported provide fresh insights into the recent experimental results in [51], and we anticipate that the findings will help interpret future experimental results not only in ecological systems, but also in biological, neuronal and physical systems where the system dynamics are represented by complex networks of coupled nonlinear oscillators and pattern switching plays a key role in the system functions.

METHODS

The stability of the cluster synchronization states can be analyzed by means of the conditional Lyapunov exponent. The key to the emergence of cluster synchronization lies in the symmetry of the network, based on which the original network can be reduced [53]. In Fig. 7(a) we present one example,

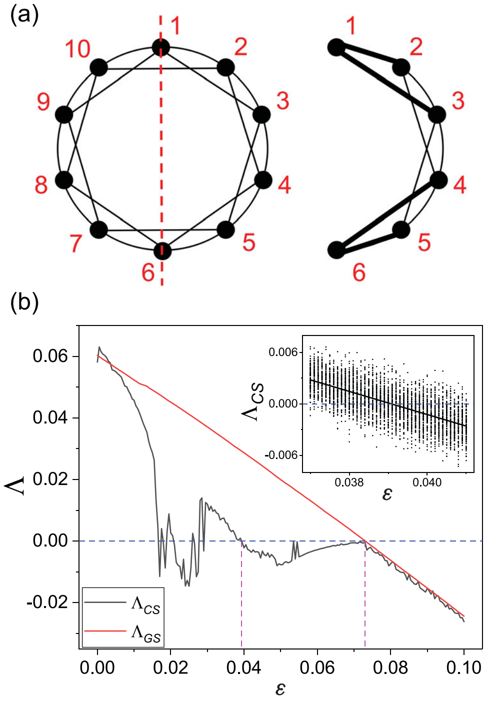

Figure 7. Network symmetry and conditional Lyapunov exponent determining the stability of cluster synchronization. (a) The original (left) and reduced network (right). The red dashed line specifies one of the symmetry axes. The reduced network is weighted, where the thickness of an edge indicates the corresponding weight. (b) The conditional Lyapunov exponent Λ_{CS} quantifying the stability of cluster synchronization versus ε (the gray curve). The transverse Lyapunov exponent Λ_{GS} characterizes the stability of global synchronization (the red curve). Both exponents are calculated using a long time interval (10^5). The pink vertical dashed line at $\varepsilon \approx 0.039 \equiv \varepsilon_c^{CS}$ is the critical coupling above which the cluster synchronization is stable, while that at $\varepsilon \approx 0.073 \equiv \varepsilon_c^{GS}$ is the transition point to stable global synchronization. The inset shows the values of Λ_{CS} calculated in finite time (10^3) with 100 realizations, and the solid black line is the linear fit of the data points. When the coupling parameter is in the vicinity of ε_c^{CS}, intermittent cluster synchronization can emerge. For $\varepsilon \lesssim \varepsilon_c^{CS}$, because Λ_{CS} is slightly positive, intermittency can be observed without external noise (cf. Fig. 2). For $\varepsilon \gtrsim \varepsilon_c^{CS}$, because of the negativity of Λ_{CS}, cluster synchronization is stable but intermittency can still arise when there is external noise of reasonably large amplitude.

where the symmetry axis is the line connecting nodes 1 and 6 in the original network (the left panel). In this case, the four nodes on the left-hand side of the symmetry axis are equivalent to their respective mirror counterparts on the right-hand side, generating four pairs (clusters) of synchronous nodes: 2 and 10, 3 and 9, 4 and 8, as well as 5 and 7. The network is thus equivalent to a reduced network with six independent nodes, as shown in the right panel of Fig. 7(a), where the edges in the reduced network are weighted [53]. The reduced network defines the dynamics of the synchronization manifold

$$\dot{\mathbf{X}} = \mathbf{F} + \varepsilon \mathcal{M} \cdot \mathbf{H}, \tag{3}$$

where $\mathcal{M}$ is the coupling matrix of the reduced network, $\mathbf{X}$, $\mathbf{F}$ and $\mathbf{H}$ are respectively the state vector, the velocity fields of isolated nodal dynamics and the coupling function.

Let $\delta\mathbf{X}$ be infinitesimal perturbations transverse to the cluster synchronization manifold, whose evolution is governed by the variational equation

$$\delta\dot{\mathbf{X}} = (\mathcal{DF} + \varepsilon \mathcal{L} \cdot \mathcal{DH}) \cdot \delta\mathbf{X}, \tag{4}$$

where $\mathcal{L}$ is the transverse Laplacian matrix, and $\mathcal{DF}$ and $\mathcal{DH}$ are the Jacobian matrices of the isolated nodal dynamics and of the coupling function, respectively. Combining equations (3) and (4), we can calculate the largest transverse Lyapunov exponent Λ_{CS} (or the conditional Lyapunov exponent), which depends on the coupling parameter ε. The necessary condition for the cluster synchronous state to be stable is $\Lambda_{CS} < 0$. In Fig. 7(b) we show Λ_{CS} as a function of ε (the solid gray curve). Also shown is the transverse Lyapunov exponent Λ_{GS} determining the stability of global synchronization (solid red curve). The wild fluctuations of Λ_{CS} in the interval $\varepsilon \in (0.015, 0.03)$ are due to the occurrence of periodic windows together with transient chaos [54]. Transition to stable cluster synchronization occurs at $\varepsilon \approx 0.039 \equiv \varepsilon_c^{CS}$, and transition to global (phase and amplitude) synchronization occurs at $\varepsilon \approx 0.073 \equiv \varepsilon_c^{GS}$.

For $\varepsilon \lesssim \varepsilon_c^{CS}$, cluster synchronization is asymptotically unstable. However, there are epochs of time during which the synchronous dynamics are stable, as indicated by the spread in the values of the conditional Lyapunov exponent calculated in finite time (e.g. 10^3) into the negative side, as can be seen from the inset in Fig. 7(b). For $\varepsilon = 0.038$, the asymptotic value of Λ_{CS} is close to zero. The probabilities for the value of the finite-time exponent $\Lambda_{CS}(t)$ to be positive and negative are thus approximately equal. The dynamics of cluster synchronization can then be treated as an unbiased random walk. For such a stochastic process, the distribution of the first passage time [55] is algebraic with scaling exponent 1.5, which explains the scaling exemplified in Fig. 3. When external noise is present, the underlying random walk process becomes biased. In this case, the scaling exponent of the transient cluster synchronization time deviates from 1.5, as demonstrated in Fig. 4.

A full description of the methods is given in Section II of the SM.

DATA AVAILABILITY

All relevant data are available from the authors upon request.

CODE AVAILABILITY

All relevant computer codes are available from the authors upon request.

SUPPLEMENTARY DATA

Supplementary data are available at *NSR* online.

FUNDING

We acknowledge support from the Vannevar Bush Faculty Fellowship program sponsored by the Basic Research Office of the Assistant Secretary of Defense for Research and Engineering and funded by the Office of Naval Research through Grant No. N00014-16-1-2828. H.W.F. and X.G.W. were supported by the National Natural Science Foundation of China (11875182).

AUTHOR CONTRIBUTIONS

Y.C.L. and H.W.F. conceived the project. H.W.F. and L.W.K. performed the computations and analysis. All authors analyzed the data. Y.C.L. wrote the paper with help from H.W.F. and X.G.W.

Conflict of interest statement. None declared.

REFERENCES

1. Earn DJD, Rohani P and Grenfell B. Persistence, chaos and synchrony in ecology and epidemiology. *Proc R Soc Lond B* 1998; **265**: 7–10.
2. Blasius B, Huppert A and Stone L. Complex dynamics and phase synchronization in spatially extended ecological systems. *Nature* 1999; **399**: 354–9.
3. Blasius B and Stone L. Chaos and phase synchronization in ecological systems. *Int J Bif Chaos* 2000; **10**: 2361–80.
4. Harrison MA, Lai YC and Holt RD. A dynamical mechanism for coexistence of dispersing species without trade-offs in spatially extended ecological systems. *Phys Rev E* 2001; **63**: 051905.
5. Harrison MA, Lai YC and Holt RD. Dynamical mechanism for coexistence of dispersing species. *J Theor Biol* 2001; **213**: 53–72.
6. Stone L, Olinky R and Blasius B *et al.* Complex synchronization phenomena in ecological systems. *AIP Conf Proc* 2002; **633**: 476–87.
7. Stone L, He D and Becker K *et al.* Unusual synchronization of red sea fish energy expenditures. *Ecol Lett* 2003; **6**: 83–6.
8. Goldwyna EE and Hastings A. When can dispersal synchronize populations? *Theor Popul Biol* 2008; **73**: 395–402.
9. Upadhyay RK and Rai V. Complex dynamics and synchronization in two non-identical chaotic ecological systems. *Chaos Solitons Fractals* 2009; **40**: 2233–41.
10. Wall E, Guichard F and Humphries AR. Synchronization in ecological systems by weak dispersal coupling with time delay. *Theor Ecol* 2013; **6**: 405–18.
11. Noble AE, Machta J and Hastings A. Emergent long-range synchronization of oscillating ecological populations without external forcing described by ising universality. *Nat Commun* 2015; **6**: 7664.
12. Giron A, Saiz H and Bacelar FS *et al.* Synchronization unveils the organization of ecological networks with positive and negative interactions. *Chaos* 2016; **26**: 065302.
13. Arumugam R and Dutta PS. Synchronization and entrainment of metapopulations: a trade-off among time-induced heterogeneity, dispersal, and seasonal force. *Phys Rev E* 2018; **97**: 062217.
14. Noble AE, Rosenstock TS and Brown PH *et al.* Spatial patterns of tree yield explained by endogenous forces through a correspondence between the ising model and ecology. *Proc Natl Acad Sci USA* 2018; **115**: 1825–30.
15. Elton C and Nicholson M. The ten-year cycle in numbers of the lynx in canada. *J Anim Ecol* 1942; **11**: 215–44.
16. Moran PAP. The statistical analysis of the Canadian lynx cycle. *Aust J Zool* 1953; **1**: 291–8.
17. Bulmer MG. A statistical analysis of the 10-year cycle in Canada. *J Anim Ecol* 1974; **43**: 701–8.
18. Schaffer W. Stretching and folding in lynx fur returns: evidence for a strange attractor in nature? *Am Nat* 1984; **124**: 798–820.
19. Ranta E, Kaitala V and Lundberg P. The spatial dimension in population fluctuations. *Science* 1997; **278**: 1621–3.
20. Hastings A and Higgins K. Persistence of transients in spatially structured ecological models. *Science* 1994; **263**: 1133–6.
21. Hastings A. Transient dynamics and persistence of ecological systems. *Ecol Lett* 2001; **4**: 215–20.
22. Dhamala M, Lai YC and Holt R. How often are chaotic transients in spatially extended ecological systems? *Phys Lett* 2001; **280**: 297–302.
23. Hastings A. Transients: the key to long-term ecological understanding? *Trends Ecol Evol* 2004; **19**: 39–45.
24. Hastings A. Timescales and the management of ecological systems. *Proc Natl Acad Sci USA* 2016; **113**: 14568–73.
25. Hastings A, Abbott KC and Cuddington K *et al.* Transient phenomena in ecology. *Science* 2018; **361**: eaat6412.
26. Rosenblum MG, Pikovsky AS and Kurths J. Phase synchronization of chaotic oscillators. *Phys Rev Lett* 1996; **76**: 1804–7.
27. Ao B and Zheng Z. Partial synchronization on complex networks. *Europhys Lett* 2006; **74**: 229.
28. Fu C, Deng Z and Huang L Topological control of synchronous patterns in systems of networked chaotic oscillators. *Phys Rev E* 2013; **87**: 032909.
29. Nicosia V, Valencia M and Chavez M *et al.* Remote synchronization reveals network symmetries and functional modules. *Phys Rev Lett* 2013; **110**: 174102.
30. Pecora LM, Sorrentino F and Hagerstrom AM *et al.* Cluster synchronization and isolated desynchronization in complex networks with symmetries. *Nat Commun* 2014; **5**: 4079.

31. Wang X, Guan S and Lai YC *et al.* Desynchronization and on-off intermittency in complex networks. *Europhys Lett* 2009; **88**: 28001.
32. Zanette DH and Mikhailov AS. Dynamical clustering in large populations of Rössler oscillators under the action of noise. *Phys Rev E* 2000; **62**: R7571.
33. Stone L and He DH. Chaotic oscillations and cycles in multi-trophic ecological systems. *J Theor Biol* 2007; **248**: 382–90.
34. Holland MD and Hastings A. Strong effect of dispersal network structure on ecological dynamics. *Nature* 2008; **456**: 792–4.
35. Feudel U, Grebogi C and Hunt BR *et al.* Map with more than 100 coexisting low-period periodic attractors. *Phys Rev E* 1996; **54**: 71–81.
36. Feudel U and Grebogi C. Multistability and the control of complexity. *Chaos* 1997; **7**: 597–604.
37. Kraut S, Feudel U and Grebogi C. Preference of attractors in noisy multistable systems. *Phys Rev E* 1999; **59**: 5253–60.
38. Kraut S and Feudel U. Multistability, noise, and attractor hopping: the crucial role of chaotic saddles. *Phys Rev E* 2002; **66**: 015207.
39. Feudel U and Grebogi C. Why are chaotic attractors rare in multistable systems? *Phys Rev Lett* 2003; **91**: 134102.
40. Ngonghala CN, Feudel U and Showalter K. Extreme multistability in a chemical model system. *Phys Rev E* 2011; **83**: 056206.
41. Patel MS, Patel U and Sen A *et al.* Experimental observation of extreme multistability in an electronic system of two coupled Rössler oscillators. *Phys Rev E* 2014; **89**: 022918.
42. Pisarchik AN and Feudel U. Control of multistability. *Phys Rep* 2014; **540**: 167–218.
43. Lai YC and Grebogi C. Quasiperiodicity and suppression of multistability in nonlinear dynamical systems. *Euro Phys J Spec Top* 2017; **226**: 1703–19.
44. Hastings A and Powell T. Chaos in a three-species food chain. *Ecology* 1991; **72**: 896–903.
45. Rosenzweig ML and MacArthur RH. Graphical representation and stability conditions of predator-prey interactions. *Am Nat* 1963; **97**: 209–23.
46. Barahona M and Pecora LM. Synchronization in small-world systems. *Phys Rev Lett* 2002; **89**: 054101.
47. Hong H, Choi MY and Kim BJ. Synchronization on small-world networks. *Phys Rev E* 2002; **65**: 026139.
48. Nishikawa T, Motter AE and Lai YC *et al.* Heterogeneity in oscillator networks: are smaller worlds easier to synchronize? *Phys Rev Lett* 2003; **91**: 014101.
49. Fu C, Lin W and Huang L *et al.* Synchronization transition in networked chaotic oscillators: the viewpoint from partial synchronization. *Phys Rev E* 2014; **89**: 052908.
50. Cao B, Wang YF and Wang L *et al.* Cluster synchronization in complex network of coupled chaotic circuits: an experimental study. *Front Phys* 2018; **13**: 130505.
51. Blasius B, Rudolf L and Weithoff G *et al.* Long-term cyclic persistence in an experimental predator-prey system. *Nature* 2020; **577**: 226–30.
52. Hastings A. Predator-prey cycles achieved at last. *Nature* 2020; **577**: 172–3.
53. Lin W, Fan H and Wang Y *et al.* Controlling synchronous patterns in complex networks. *Phys Rev E* 2016; **93**: 042209.
54. Lai YC and Tél T. *Transient Chaos—Complex Dynamics on Finite Time Scales*. New York: Springer, 2011.
55. Ding M and Yang W. Distribution of the first return time in fractional Brownian motion and its application to the study of on-off intermittency. *Phys Rev E* 1995; **52**: 207–13.

Supplementary Information for

Synchronization within synchronization: transients and intermittency in ecological networks

Huawei Fan, Ling-Wei Kong, Xingang Wang, Alan Hastings, and Ying-Cheng Lai*

CONTENTS

I. STABILITY ANALYSIS OF CLUSTER SYNCHRONIZATION

Let $\mathcal{S}$ be the permutation symmetry that the network possesses and $\mathbf{X}_s$ be a vector in the cluster synchronization manifold associated with $\mathcal{S}$. The dynamics of $\mathbf{X}_s$ are governed by

$$\frac{d\mathbf{X}_s}{dt} = \mathbf{F}(\mathbf{X}_s) + \varepsilon \mathcal{M} \cdot \mathbf{H}(\mathbf{X}_s), \tag{S1.1}$$

where $\mathbf{F}(\mathbf{x})$ is the velocity field of the isolated nodal dynamics, $\mathbf{H}(\mathbf{x})$ is the coupling function, and $\mathcal{M}$ is the coupling matrix of the reduced network. The stability of the cluster synchronization manifold is determined by the variational equation

$$\frac{d\delta\mathbf{X}}{dt} = [\mathcal{DF}(\mathbf{X}_s) + \varepsilon \mathcal{L} \cdot \mathcal{DH}(\mathbf{X}_s)] \cdot \delta\mathbf{X}, \tag{S1.2}$$

where $\delta\mathbf{X}$ is an infinitesimal perturbation transverse to the manifold, $\mathcal{L}$ is the transverse matrix determined by the network symmetry, $\mathcal{DF}(\mathbf{X}_s)$ and $\mathcal{DH}(\mathbf{X}_s)$ are the Jacobian matrices of the velocity field and of the coupling function evaluated at $\mathbf{X}_s$, respectively. For the cluster synchronization state to be stable, the necessary condition is that $\delta\mathbf{X}$ approaches zero exponentially with time. Let Λ be the largest Lyapunov exponent calculated from Eq. (S1.2). The stability condition is $\Lambda < 0$.

The coupling matrix $\mathcal{M}$ is constructed according to the network symmetry $\mathcal{S}$, as follows. Assume the network contains n symmetric nodal pairs (the symmetric group) and m "isolated" nodes that are not connected with any node in the symmetric group. The number of nodes in the reduced network is $N' = n + m$, in which the coupling strength that node l receives from node k can be written as

$$\mathcal{M}_{lk} = (\sum_{i \in v_l} \sum_{j \in v_k} a_{ij})/q,$$

where v_l (or v_k) is the set of symmetric nodes in the original network which are represented by node l (or k) in the reduced network, $\mathcal{A} = \{a_{ij}\}$ is the adjacency matrix of the original network, and $q = 2$ (or $q = 1$) if node i belongs to a symmetric pair (or is an isolated node). The transverse matrix $\mathcal{L}$ in Eq. (S1.2) is obtained by transforming the matrix $\mathcal{A}$ into the space spanned by the eigenvectors of the network symmetry matrix $\mathcal{P} = \{p_{ij}\}$, as follows. If nodes i and j are symmetric in the network, we set $p_{ij} = p_{ji} = 1$; if node i is isolated, we set $p_{ii} = 1$; the remaining elements are all set as zero. Let $\mathcal{T}$ be the transformation matrix constructed from the eigenvectors of $\mathcal{P}$, which can be applied to the coupling matrix $\mathcal{G} = \mathcal{A} - \mathcal{K}$ to yield a matrix in the blocked form:

$$\mathcal{G}' = \mathcal{T}^{-1} \cdot \mathcal{G} \cdot \mathcal{T} = \begin{pmatrix} \mathcal{B} & 0 \\ 0 & \mathcal{L} \end{pmatrix}, \tag{S1.3}$$

where $\mathcal{K}$ is the diagonal matrix with elements being the degree $k_{ii} = \sum_j a_{ij}$ of node i, $\mathcal{B}$ characterizes the dynamics in the synchronization manifold (which is transformed from the coupling matrix of the reduced network, $\mathcal{M}$), and $\mathcal{L}$ is the transverse matrix that we set out to find. A straightforward way to distinguish $\mathcal{L}$ from $\mathcal{B}$ is to check which matrix gives the null eigenvalue: $\mathcal{B}$ has a null eigenvalue while $\mathcal{L}$ does not.

For the network shown in Fig. 1(a) in the main text, the symmetry axis is the line connecting nodes 1 and 6, and the four nodes on the left side of the symmetry axis are equivalent to their respective mirror counterparts on the right side, generating four pairs (clusters) of synchronous nodes: 2 and 10, 3 and 9, 4 and 8, as well as 5 and 7. Hence, the cluster synchronization manifold is defined by $\mathbf{x}_1 \equiv \mathbf{x}_1^s$, $\mathbf{x}_2 = \mathbf{x}_{10} \equiv \mathbf{x}_{2,10}^s$, $\mathbf{x}_3 = \mathbf{x}_9 \equiv \mathbf{x}_{3,9}^s$, $\mathbf{x}_4 = \mathbf{x}_8 \equiv \mathbf{x}_{4,8}^s$, $\mathbf{x}_5 = \mathbf{x}_7 \equiv \mathbf{x}_{5,7}^s$, and $\mathbf{x}_6 \equiv \mathbf{x}_6^s$ where $\mathbf{x}_i$ is the vector of the dynamical variables of node i. More specifically, the vector $\mathbf{X}_s$ in the synchronization manifold, the velocity field $\mathbf{F}$ and the coupling function $\mathbf{H}$ in Eq. (S1.1) are

$$\begin{aligned}
\mathbf{X}_s &= [(\mathbf{x}_1^s)^T, (\mathbf{x}_{2,10}^s)^T, (\mathbf{x}_{3,9}^s)^T, (\mathbf{x}_{4,8}^s)^T, (\mathbf{x}_{5,7}^s)^T, (\mathbf{x}_6^s)^T]^T, \\
\mathbf{F} &= [(\mathbf{F}(\mathbf{x}_1^s))^T, (\mathbf{F}(\mathbf{x}_{2,10}^s))^T, (\mathbf{F}(\mathbf{x}_{3,9}^s))^T, (\mathbf{F}(\mathbf{x}_{4,8}^s))^T, (\mathbf{F}(\mathbf{x}_{5,7}^s))^T, (\mathbf{F}(\mathbf{x}_6^s))^T]^T, \\
\mathbf{H} &= [(\mathbf{H}(\mathbf{x}_1^s))^T, (\mathbf{H}(\mathbf{x}_{2,10}^s))^T, (\mathbf{H}(\mathbf{x}_{3,9}^s))^T, (\mathbf{H}(\mathbf{x}_{4,8}^s))^T, (\mathbf{H}(\mathbf{x}_{5,7}^s))^T, (\mathbf{H}(\mathbf{x}_6^s))^T]^T,
\end{aligned}$$

In the cluster synchronization state, the dynamics of the network are equivalent to the dynamics of a reduced network with $N' = 6$ independent nodes, as shown in the right panel of Fig. 7(a) in the main text. The coupling matrix of the reduced network is

$$\mathcal{M} = \begin{bmatrix} -4 & 2 & 2 & 0 & 0 & 0 \\ 1 & -3 & 1 & 1 & 0 & 0 \\ 1 & 1 & -4 & 1 & 1 & 0 \\ 0 & 1 & 1 & -4 & 1 & 1 \\ 0 & 0 & 1 & 1 & -3 & 1 \\ 0 & 0 & 0 & 2 & 2 & -4 \end{bmatrix}. \tag{S1.4}$$

The permutation matrix associated with the network symmetry is

$$\mathcal{P} = \begin{bmatrix} 1&0&0&0&0&0&0&0&0&0 \\ 0&0&0&0&0&0&0&0&0&1 \\ 0&0&0&0&0&0&0&0&1&0 \\ 0&0&0&0&0&0&0&1&0&0 \\ 0&0&0&0&0&0&1&0&0&0 \\ 0&0&0&0&0&1&0&0&0&0 \\ 0&0&0&0&1&0&0&0&0&0 \\ 0&0&0&1&0&0&0&0&0&0 \\ 0&0&1&0&0&0&0&0&0&0 \\ 0&1&0&0&0&0&0&0&0&0 \end{bmatrix}. \tag{S1.5}$$

Transforming the coupling matrix of the original network to the space spanned by the eigenvectors of $\mathcal{P}$, we obtain the transverse matrix

$$\mathcal{L} = \begin{bmatrix} -5 & 1 & 1 & 0 \\ 1 & -4 & 1 & 1 \\ 1 & 1 & -4 & 1 \\ 0 & 1 & 1 & -5 \end{bmatrix}, \tag{S1.6}$$

which is used in Eq. (S1.2) for calculating the conditional Lyapunov exponent Λ plotted in Fig. 7 in the main text.

Altogether, in addition to the case shown in Fig. 1(a) in the main text, the network has four other reflection symmetries, with axes being the lines connecting nodal pairs $(4,9)$, $(5,10)$, $(3,8)$, and $(2,7)$, respectively, each generating a distinct pattern of cluster synchronization, as demonstrated in Fig. 2 in the main text. The stability of the corresponding synchronization manifold can be analyzed in a similar manner.

II. CLUSTER AND GLOBAL SYNCHRONIZATION FOR NONIDENTICAL COUPLING

We study the general case where the coupling parameters associated with herbivores and predators are not identical: $\varepsilon_y \neq \varepsilon_z$. We focus on the values of the two transverse Lyapunov exponents: Λ_{CS} and Λ_{GS}, which determine the stability of cluster and global synchronization in the network, respectively. Figure S1(a) shows the color coded values of Λ_{CS} in the parameter plane $(\varepsilon_y, \varepsilon_z)$, where the value of Λ_{CS} mostly decreases with ε_y and varying the value of ε_z has little effect on the exponent. For instance, the black curve representing the contour of $\Lambda_{CS} = 0$ and therefore separating the synchronization and desynchronization regions is almost vertical and located about $\varepsilon_y \approx 0.04$. This behavior implies that the coupling among the herbivores is more important than that among the predators for cluster synchronization. For global synchronization, it is convenient to use the generalized coupling parameters: $K_y = \lambda\varepsilon_y$ and $K_z = \lambda\varepsilon_z$, where λ is the eigenvalue of the Laplacian matrix of the network. The color coded values of Λ_{GS} are shown in Fig. S1(b). It can be seen that the coupling among the herbivores also plays an important role in global synchronization of the whole network.

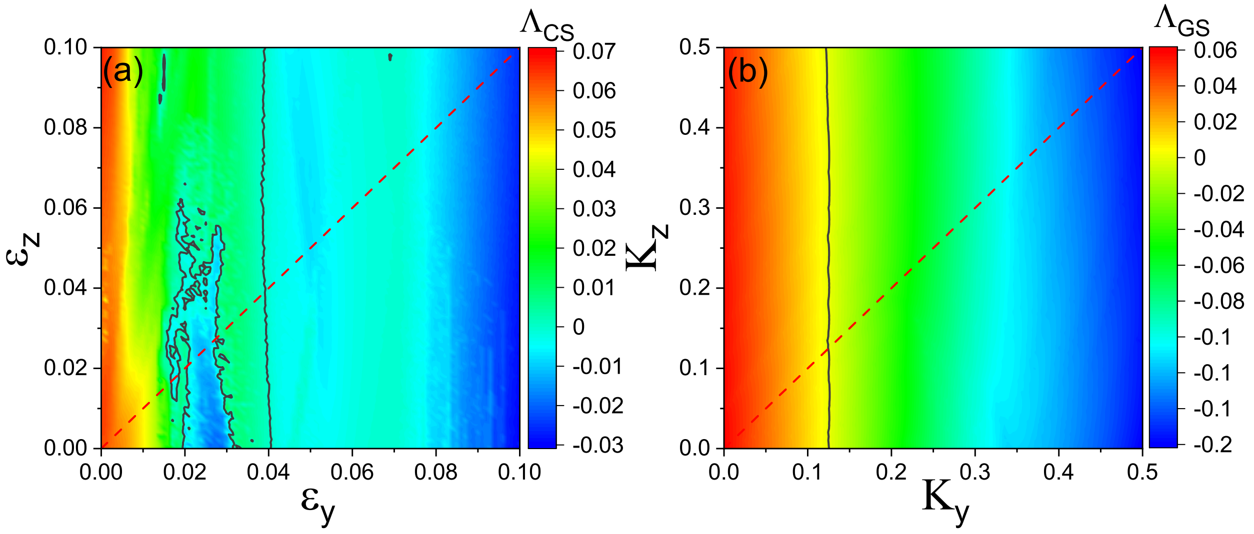

FIG. S1. *Cluster and global synchronization for nonidentical values of the coupling parameters associated with herbivores and predators.* (a) Values of the conditional Lyapunov exponent Λ_{CS} characterizing cluster synchronization in the parameter plane $(\varepsilon_y, \varepsilon_z)$, and (b) values of the transverse Lyapunov exponent Λ_{GS} for global synchronization (in both phase and amplitude) in the plane of the generalized coupling parameters (K_y, K_z). In each panel, the mostly vertical black curve is the contour along which the value of the corresponding exponent is zero.

III. FLUCTUATIONS OF THE FINITE TIME LYAPUNOV EXPONENT

The top panel of Fig. S2 demonstrates explicitly the fluctuations of the finite time Lyapunov exponent for $\varepsilon = 0.038$, where the exponent Λ_{CS} is calculated in a short time interval $\Delta t = 10^{-2}$ so that it can be regarded as a continuous function of time. For reference, the corresponding time evolution of all species populations in the network are shown (in the three lower panels). It can be seen that, in any one cycle of population oscillation, Λ_{CS} possesses both positive and negative values, making its asymptotic value approximately zero. In this case, cluster synchronization can be maintained but for a finite amount of time - arbitrarily small uncertainties or perturbations (e.g., inevitable computational errors) can drive the network out of the specific cluster synchronization state and make it approach another coexisting state, generating intermittency as demonstrated in Fig. 2 in the main text.

A noticeable feature of the finite time conditional Lyapunov exponent $\Lambda_{CS}(t)$, as shown in Fig. S2, is that its negative peaks are relatively sharp and each corresponds to the position of a near maximum for $y_i(t)$ and $z_i(t)$, as indicated by the vertical red dashed lines in Fig. S2. This indicates that the system tends to synchronize when the herbivore and predator populations begin to decay.

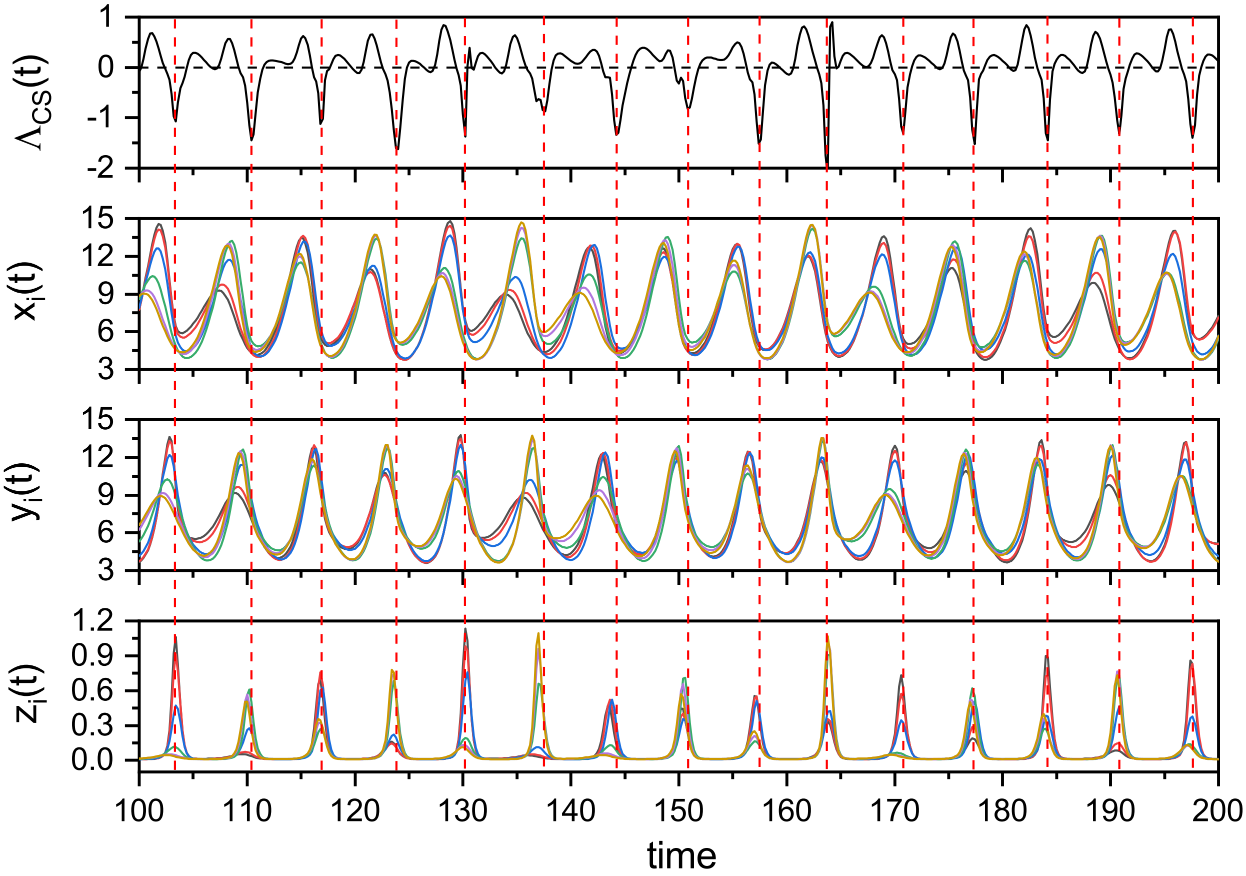

FIG. S2. *Time evolution of the finite time conditional Lyapunov exponent* $\Lambda_{CS}(t)$. The four panels (from top down) correspond to $\Lambda_{CS}(t)$ and the evolution of species populations x_i, y_i, and z_i in all patches (distinguished by different colors). The coupling parameter is $\varepsilon = 0.038$ - the same value as in Fig. 2 in the main text.

IV. TRANSIENTS AND INTERMITTENT SYNCHRONIZATION IN A NETWORK OF ODD NUMBER OF PATCHES

We consider a spatial network of $n = 11$ patches. Different from the case of an even number of patches, here the network has 6 symmetry axes and, for each axis, there are 5 symmetric nodal pairs and one isolated node (node 1). The upper panel of Fig. S3 shows the network structure. Representative time evolution of the matrix elements c_{ij} is shown in the lower panel of Fig. S3 (for $\varepsilon = 0.05$). As in the network of an even number of patches treated in the main text, the phenomena of cluster synchronization shadowed by chaotic phase synchronization and intermittency persist for networks with an odd number of patches.

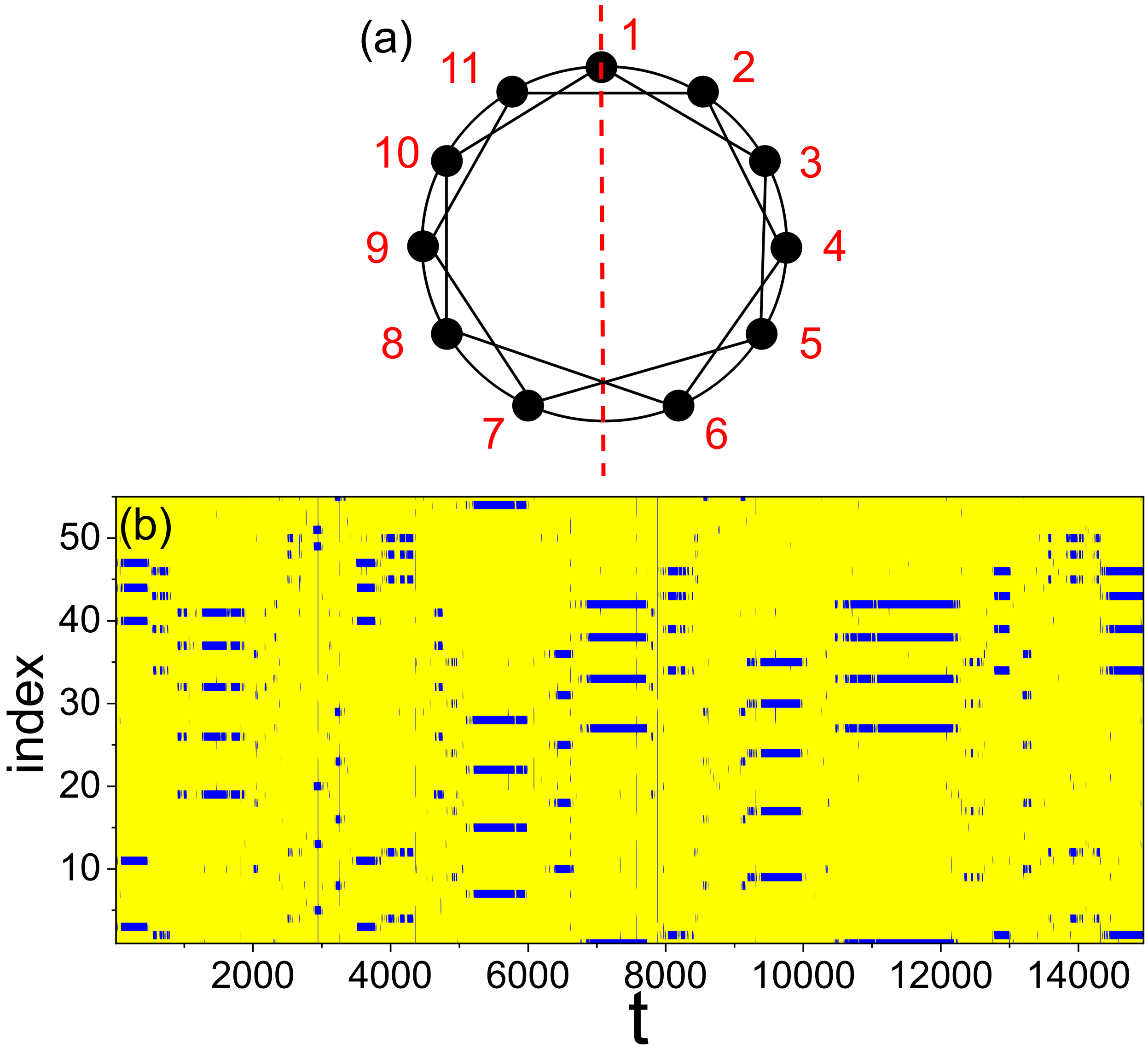

FIG. S3. *Structure and intermittent cluster synchronization in a network of odd number of patches.* (a) A dispersal network of eleven patches with a regular ring structure. The red dotted line specifies one of the symmetry axes. (b) Time evolution of the matrix elements $c_{ij}(t)$ for $\varepsilon = 0.05$.

V. TRANSIENTS AND INTERMITTENT SYNCHRONIZATION IN A TWO-DIMENSIONAL LATTICE OF PATCHES

We study a two-dimensional lattice of patches, as shown in the upper panel of Fig. S4. The network size is $n = 16$ with periodic boundary conditions. The lower panel in Fig. S4 shows the time evolution of the matrix elements c_{ij} in a long time interval of approximately 60000 average periods. In spite of the spatially two-dimensional structure of the network, the phenomena of cluster synchronization umbrellaed by chaotic phase synchronization and intermittent switching among distinct cluster synchronization patterns still occur.

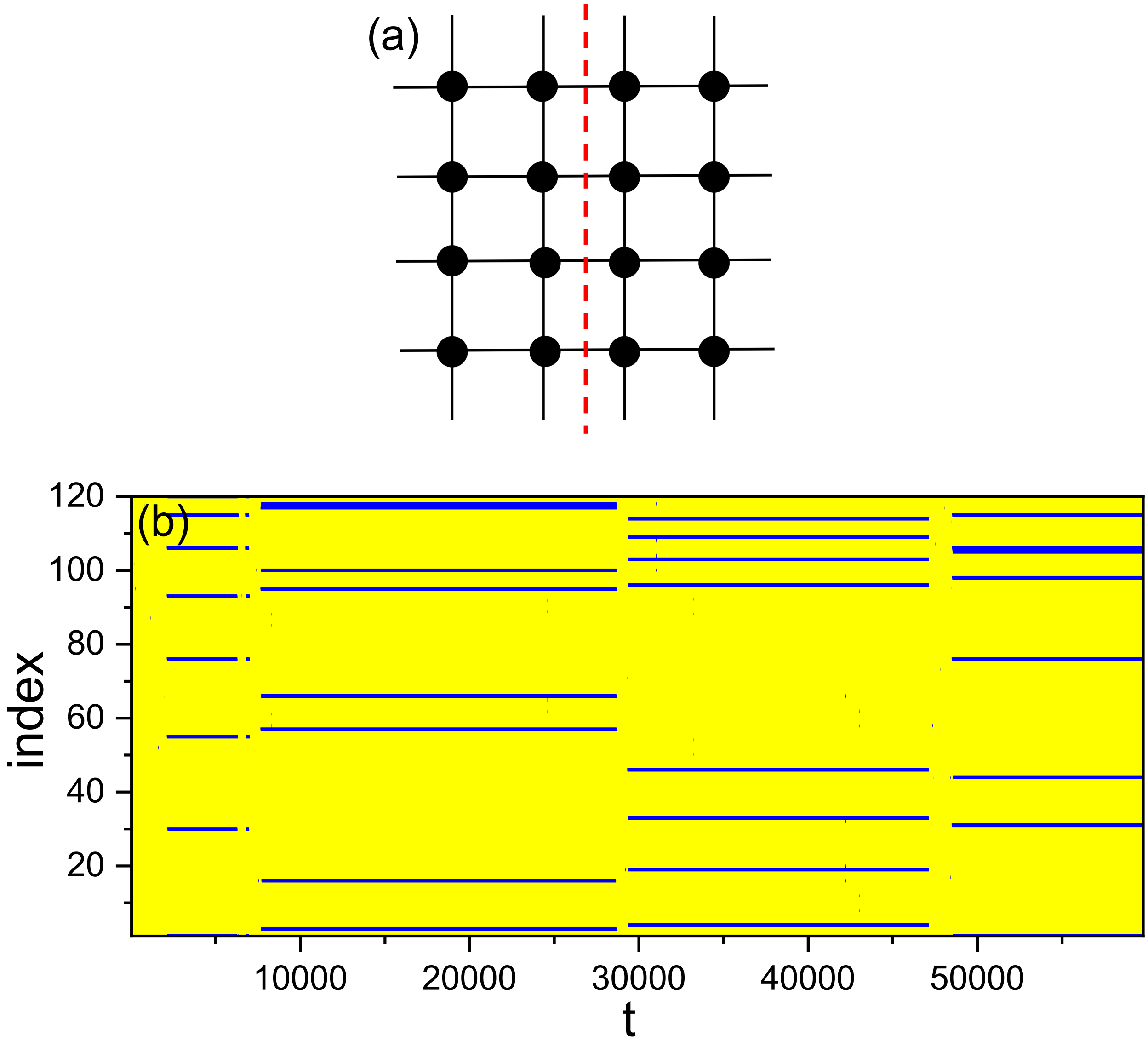

FIG. S4. *Network structure and intermittent cluster synchronization in a two-dimensional spatial lattice of patches.* (a) A dispersal network of sixteen patches with a two-dimensional lattice structure. The red dotted line specifies one of the symmetry axes. (b) The time evolution of the matrix elements $c_{ij}(t)$ for $\varepsilon = 0.0257$.

VI. EFFECT OF COUPLING ON TRANSIENTS AND INTERMITTENCY

How does the value of the coupling parameter ε affect transient cluster synchronization and intermittency? To address this question, we calculate the evolution of the cluster synchronization matrix for a systematic set of ε values. Figure S5 shows four cases: $\varepsilon = 0.03, 0.035, 0.04$ and 0.045. For $\varepsilon \lesssim 0.03$, cluster synchronization is rare, which becomes more frequent as the value of ε is increased from 0.03. For $\varepsilon \gtrsim 0.045$, the duration of cluster synchronization becomes long: a particular state can last for a long time and numerically it becomes difficult to obtain intermittency. Nonetheless, the phenomenon of intermittent cluster synchronization can occur in a finite interval of the coupling parameter. Especially, for system (1) in the main text, the parameter interval is $0.035 \lesssim \varepsilon \lesssim 0.04$.

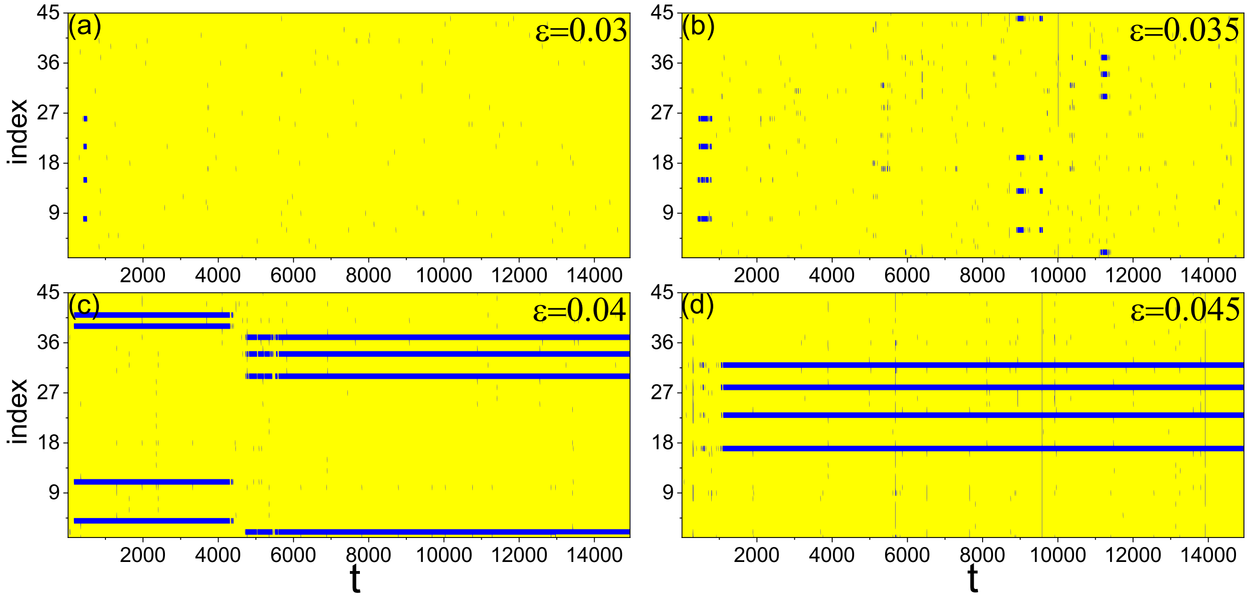

FIG. S5. *Effect of coupling on cluster synchronization.* Shown is the time evolution of the elements of the cluster synchronization matrix $c_{ij}(t)$ for (a) $\varepsilon = 0.03$, (b) $\varepsilon = 0.035$, (c) $\varepsilon = 0.04$, and (d) $\varepsilon = 0.045$. For the networked system (1) in the main text, the phenomenon of intermittent cluster synchronization occurs for $0.035 \lesssim \varepsilon \lesssim 0.04$.

VII. EFFECT OF NOISE ON TRANSIENTS AND INTERMITTENCY FOR STRONGER COUPLING

We calculate the distributions of the transient lifetime T_{CS} in a stronger coupling regime for four values of the noise amplitude, as shown in Fig. S6. In general, strong coupling leads to a longer transient lifetime, giving rise to smaller values of the algebraic exponent. For example, for $\sigma = 10^{-9}$, the exponent is $\gamma \approx 1.57$ for $\varepsilon = 0.038$. For $\varepsilon = 0.04$, the exponent has the value $\gamma \approx 1.41$.

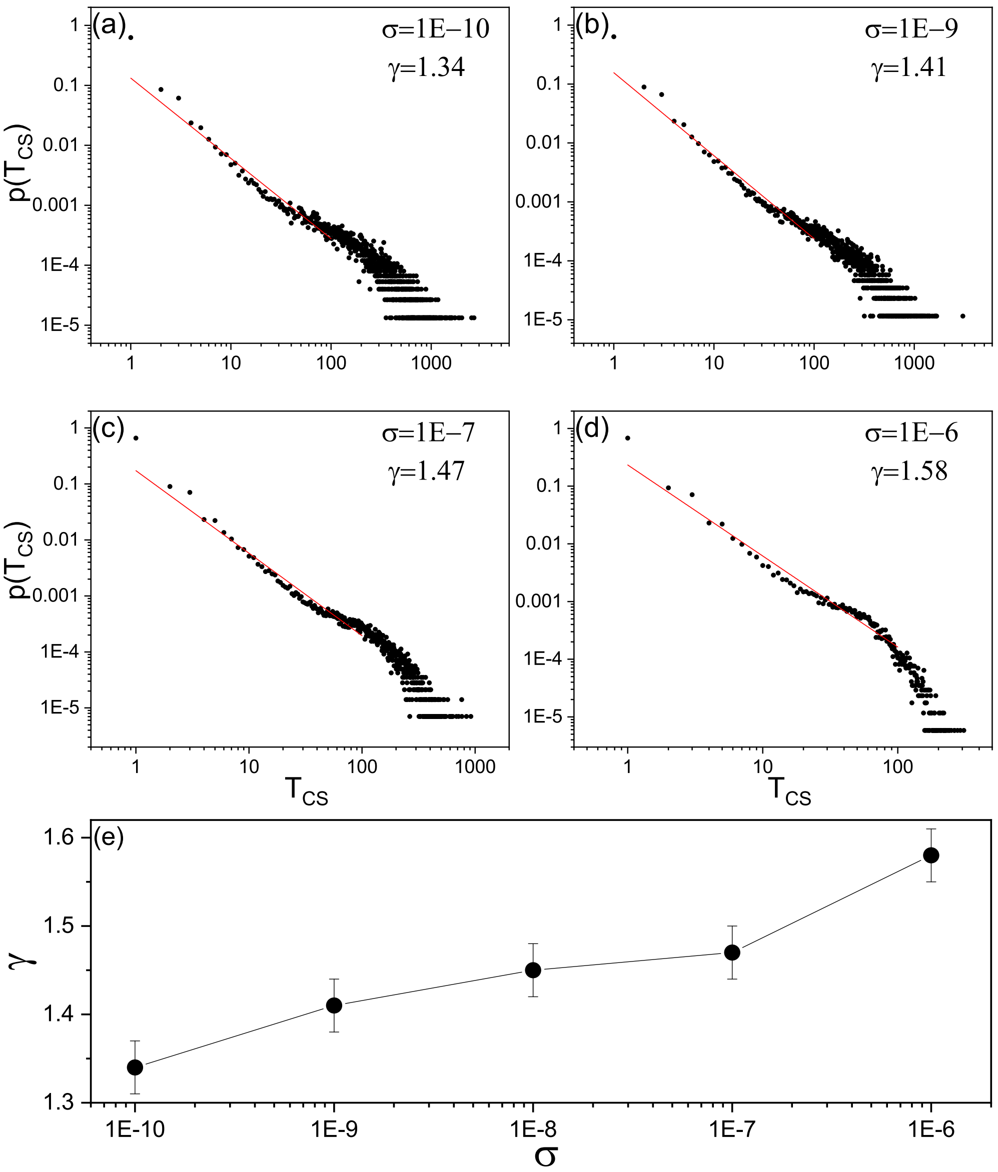

FIG. S6. *Effect of noise on algebraic distribution of the transient lifetime of cluster synchronization state.* (a-d) For $\varepsilon = 0.04$, algebraic distribution $p(T_{CS})$ for four values of noise amplitude σ: 10^{-10}, 10^{-9}, 10^{-7}, and 10^{-6}. The values of the algebraic exponent are approximately 1.34, 1.41, 1.47, and 1.58, respectively. (e) The algebraic exponent γ versus the noise amplitude σ.

VIII. TRANSIENT CLUSTER SYNCHRONIZATION FOR ALTERNATIVE VALUES OF THE LOCAL PARAMETERS

The phenomena reported in the main text have also been observed for alternative values of the parameters of the local dynamics. For example, changing the parameter b in the chaotic food web system [Eq. (1) in the main text] to 0.9 gives Fig. S7(a), the time evolution of the dynamical variables. It can be seen that, similar to the results in the main text [Fig. 2], the time evolution is characteristic of the phenomenon of intermittent cluster synchronization. This is also the case for the Hastings-Powell system. In particular, setting $d_1 = 0.35$ and $\varepsilon = 0.025$ in Eq. (2) in the main text, we obtain Fig. S7(b), the time evolution of the dynamical variables, where intermittent cluster synchronization occurs.

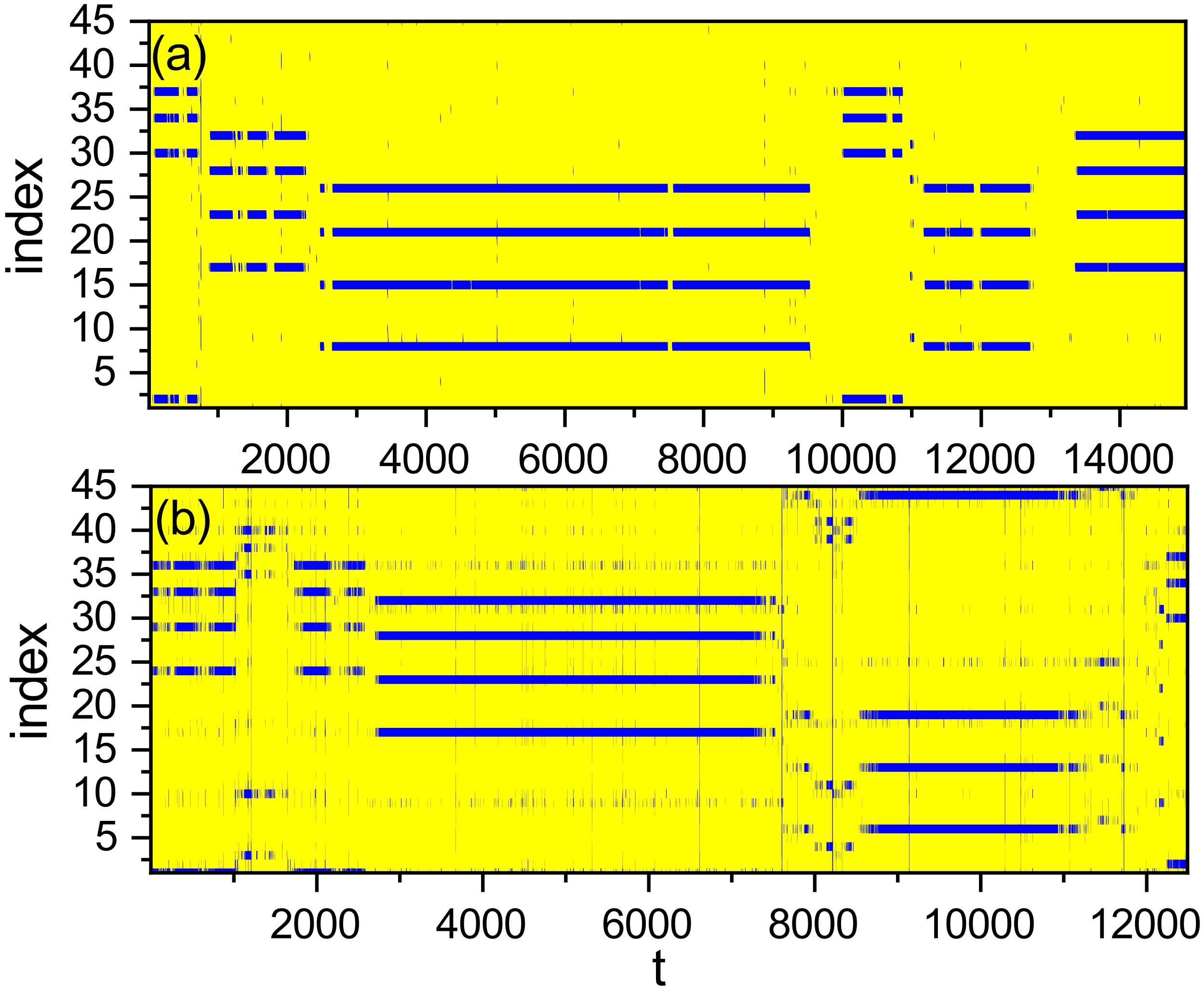

FIG. S7. *Transient cluster synchronization for alternative values of the parameters of the local nodal dynamics.* Shown is the time evolution of the dynamical variables for (a) the chaotic food web model for $b = 0.9$, and (b) the Hastings-Powell system for $d_1 = 0.35$ and $\varepsilon = 0.025$. Other parameter values are the same as those in the main text.

IX. TRANSIENT CLUSTER SYNCHRONIZATION IN COUPLED CHAOTIC RÖSSLER OSCILLATORS

Transient cluster synchronization has also been observed in networks of coupled chaotic Rössler oscillators. The network structure is identical to that in Fig. 1(a) in the main text, with the local dynamical system replaced by the classical chaotic Rössler oscillator. The network dynamical equations are

$$\begin{aligned}
\dot{x}_i &= -y_i - z_i, \\
\dot{y}_i &= x_i + a y_i + \varepsilon \sum_{j=1}^{N} a_{ij}(y_j - y_i), \\
\dot{z}_i &= z_i(x_i - c) + b,
\end{aligned}$$

where $i, j = 1, \ldots, N$ are the nodal indices, a_{ij} are the elements of the network adjacency matrix [Fig. 1(a) in the main text], and ε is the uniform coupling strength. For $(a,b,c) = (0.2, 0.2, 5.7)$, the oscillator generates a chaotic attractor. Figure S8 shows, for $\varepsilon = 0.046$, the time evolution of the synchronization relationship among the nodal dynamics. Similar to the results from the coupled ecological oscillators, the system switches randomly among different cluster synchronization states during the course of system evolution.

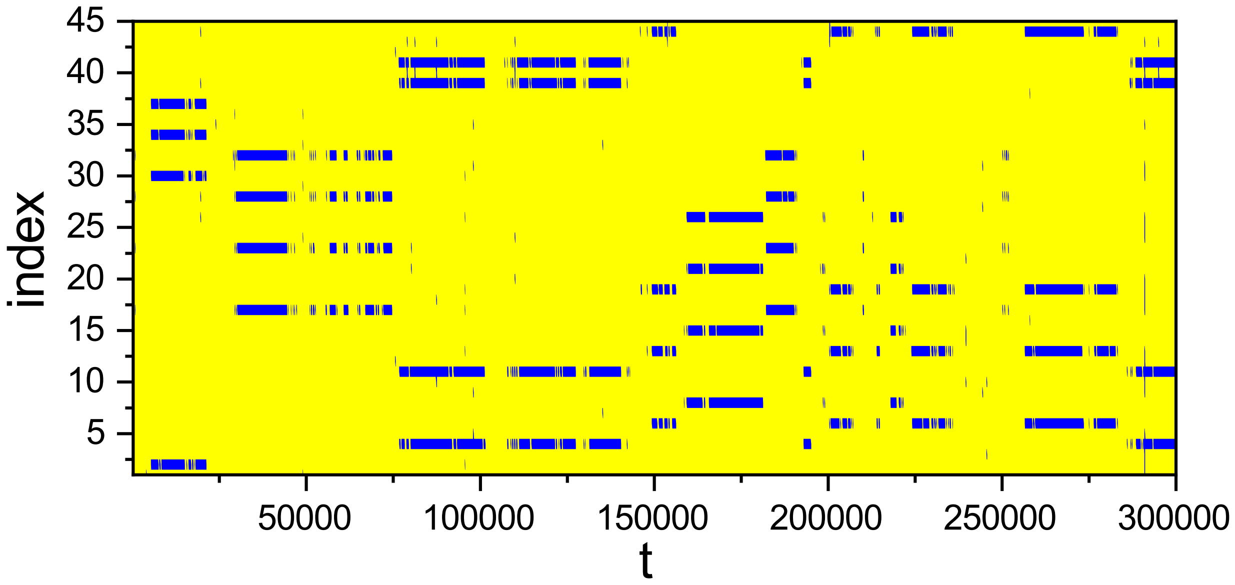

FIG. S8. *Transient cluster synchronization in coupled chaotic Rössler oscillators.* Shown is the time evolution of the synchronization relationship for coupling strength $\varepsilon = 0.046$. The network structure is identical to that in Fig. 1(a) in the main text.

X. INVERSE CUMULATIVE DISTRIBUTION OF TRANSIENT LIFETIME

To further elucidate the power-law distribution of the transient lifetime, we calculate the inverse cumulative distribution [1]. Specifically, let $f(x)$ be the probability distribution of a random variable x. The inverse cumulative distribution determines the possibility for finding an event larger than certain value of x: $P(x) = \int_x^\infty f(x)dx$. If $f(x)$ follows an algebraic scaling, we have $f(x) \sim x^\gamma$, so the inverse cumulative distribution follows an algebraic scaling: $P(x) \sim x^\Gamma$, with $\Gamma = \gamma + 1$. Figure S9 shows the cumulative distribution calculated from the same time series of transient lifetime as that in Fig. 3 in the main text. In the interval $T_{CS} \in (0, 10^2)$ (the same interval used in the main text for fitting the distribution), the distribution can be fitted by an algebraic scaling with $\Gamma \approx -0.58$. For comparison, Fig. S9 also includes the lifetime distribution shown in Fig. 3 in the main text. We have $\Gamma \approx \gamma + 1$. The thin tail in the inverse cumulative distribution is due to the limited data (a finite-size effect).

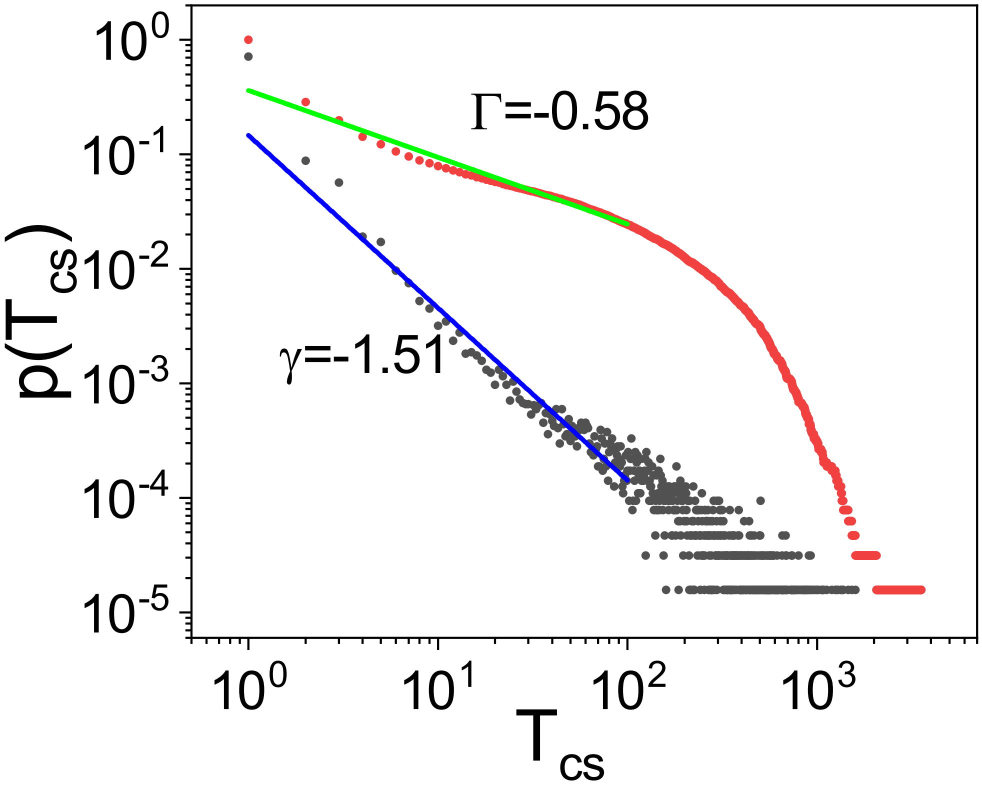

FIG. S9. *Inverse cumulative distribution of transient lifetime.* In the interval $T_{CS} \in (0, 10^2)$, the distribution can be fitted by an algebraic scaling: $p(T_{CS}) \sim T_{CS}^\Gamma$ with $\Gamma \approx -0.58$ (red dots and green line). To facilitate a comparison, the probability distribution in Fig. 3 of the the main text is also shown (black dots and blue line).

XI. VARIATION OF DEGREE OF SYNCHRONIZATION ABOUT ε_c^{CS}

For the food web network studied in the main text, in the region where transient cluster synchronization occurs, i.e, $\varepsilon \leq \varepsilon_c^{CS} \approx 0.4$, there is little change in the degree of global synchronization, as shown in Fig. S10, where the degree of synchronization is characterized the error defined as

$$\delta X = \sum_{1}^{N} [(x_i - \langle x \rangle)^2 + (y_i - \langle y \rangle)^2 + (z_i - \langle z \rangle)^2]^{1/2}/N,$$

where (x_i, y_i, z_i) is the state of the ith patch and $\langle x \rangle = \sum_i^N x_i$, $\langle y \rangle = \sum_i^N y_i$, and $\langle z \rangle = \sum_i^N z_i$ characterize the network averaged state. The behavior in in Fig. S10 is expected, as the impact of increasing the coupling strength is to extend the lifetime of the cluster synchronizations states, whereas the switchings between the different cluster synchronization states do not affect the degree of global synchronization since these states have the same δX value.

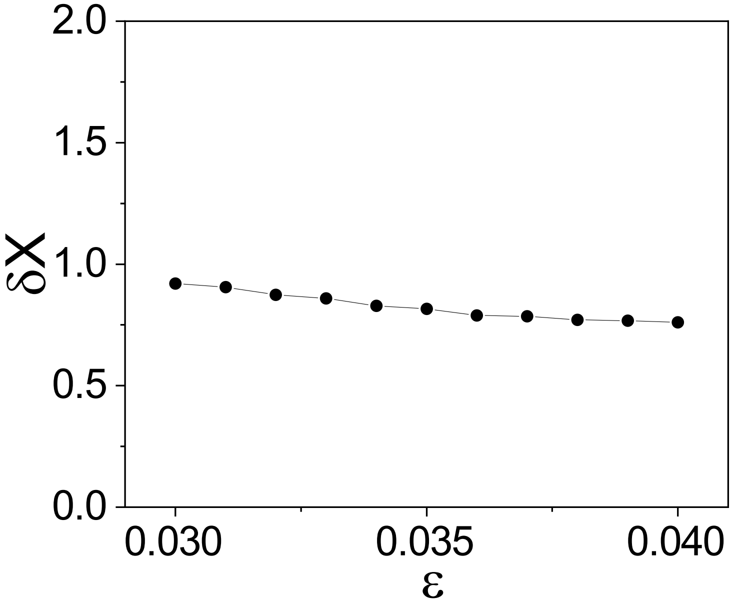

FIG. S10. *Behavior of the global synchronization error in the food web network.* Shown is δX versus ε about the critical coupling $\varepsilon_c^{CS} \approx 0.04$. In the region where transient cluster synchronization arises, i.e., $\varepsilon \in (0.035, \varepsilon_c^{CS})$, the value of δX is approximately constant. Each data point is the result of averaging over a time period of 10^4 cycles of oscillation.

XII. EFFECT OF COUPLING ON STATISTICAL PROPERTIES OF SYNCHRONIZATION MANIFOLD

Figure 7 in the main text demonstrates that, prior to the regime of transient cluster synchronization, the conditional Lyapunov exponent Λ fluctuates and crosses zero multiple times. The fluctuations are induced by the deformation of the synchronization manifold: they do not imply any new type of synchronization transition. To provide support, we show in Figs. S11 and S12 typical trajectories from patch 1 in the reduced network (Fig. 7 in the main text) for several values of the coupling strength in the fluctuating region. It can be seen that, at exactly the points where Λ becomes negative, the attractor is deformed from that of the isolated oscillator. On the contrary, in the range where transient cluster synchronization arises, i.e., $\varepsilon \in (0.035, 0.04)$, the statistical properties of the synchronization manifold are characteristically similar to those of the isolated attractor, leading to a smooth decrease in Λ with the increase of ε.

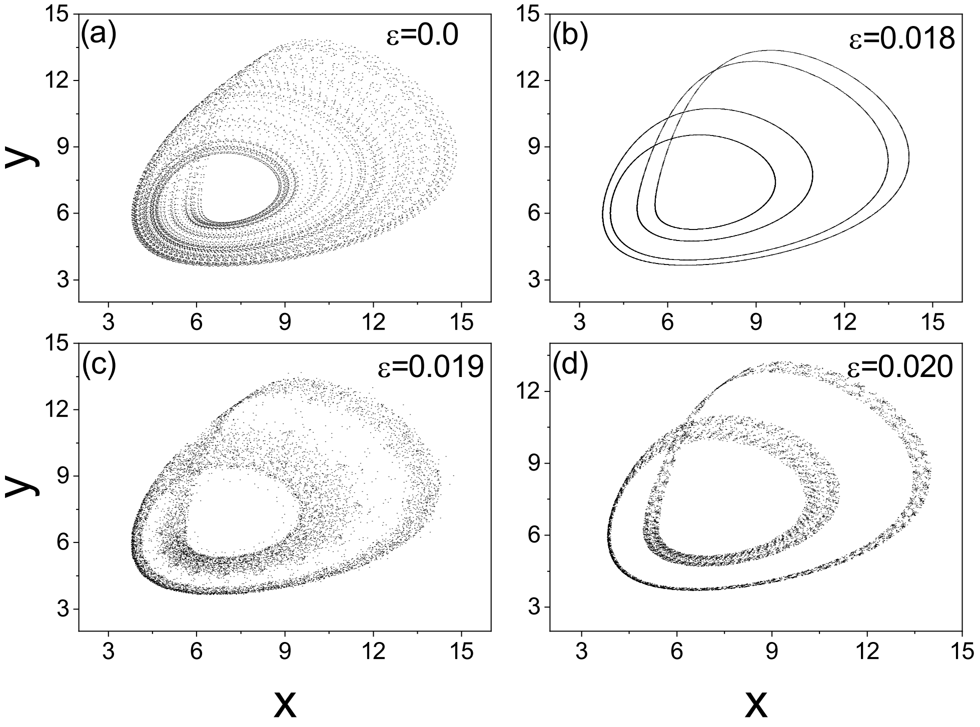

FIG. S11. *Typical trajectories from the parameter region where there are fluctuations of the conditional Lyapunov exponent.* For the chaotic food web network, in the coupling parameter range $\varepsilon \in (0.018, 0.03)$, fluctuations of the conditional Lyapunov exponent occur, due to the deformation of the synchronization manifold. Shown are typical trajectories from the first patch in the reduced network [Fig. 7(a) in the main text] for different values of the coupling strength: (a) $\varepsilon = 0$, (b) $\varepsilon = 0.018$, (c) $\varepsilon = 0.019$, and (d) $\varepsilon = 0.02$.

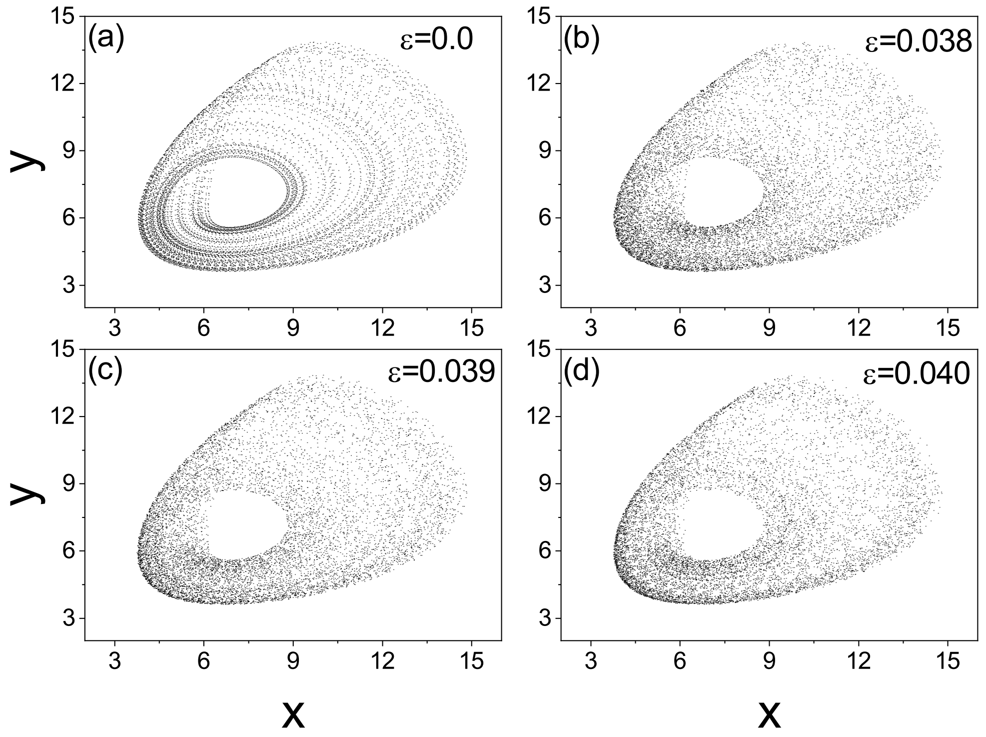

FIG. S12. *Typical trajectories from the parameter region where there is transient cluster synchronization*. For the chaotic food web network, in the parameter interval $\varepsilon \in (0.035, 0.04)$ where transient cluster synchronization arises, the synchronization manifold remains statistically unchanged. Shown are typical trajectories from the first patch in the reduced network [Fig. 7(a) in the main text] for different values of the coupling strength: (a) $\varepsilon = 0$, (b) $\varepsilon = 0.038$, (c) $\varepsilon = 0.039$, and (d) $\varepsilon = 0.04$

XIII. EFFECT OF SYMMETRY PERTURBATIONS ON TRANSIENT BEHAVIORS

Transient cluster synchronization persists when the network symmetry is slightly broken. To provide supporting evidence of the robustness of the phenomenon of transient cluster synchronization against symmetry-breaking perturbations, we introduce random perturbations of magnitude 1% to the parameter b in the chaotic food web network so that there is a slight parameter mismatch. Figure S13(a) shows the result, where the cluster synchronization states are slightly smeared, but the intermittent behavior is still apparent. Similar results are obtained when random perturbations are applied to the network couplings, as shown in Fig. S13(b), where the magnitude of the perturbations is 5% of the original value of the coupling strength.

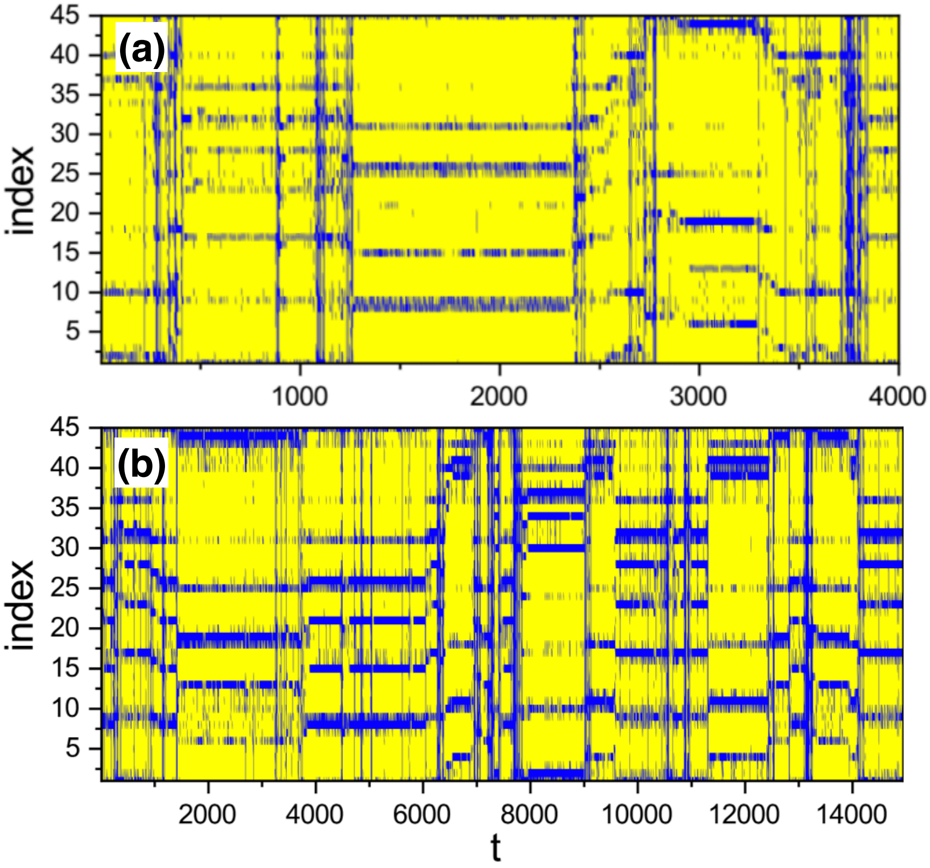

FIG. S13. *Effect of symmetry-breaking perturbations on transient cluster synchronization.* The network system is the same as the one in Figs. 1 and 2 in the main text. Shown are the time evolution of the dynamical variables of the system for $\varepsilon = 0.038$ with: (a) random perturbations of magnitude 1% in the parameter b, and (b) random perturbations of magnitude 5% in the coupling parameter.

---

[1] White, E. P., Enquist, B. J. & Green, J. L. On estimating the exponent of power-law frequency distributions. *Ecology* **89**, 905–912 (2008).